

4-2021

**TRANSCRIPTOMIC ANALYSIS OF THE GLYCOPHYTIC CROP  
Ipomoea aquatica UNDER SALINITY CONDITIONS COMPARED TO  
ITS WILD HALOPHYTE RELATIVE Ipomoea pes-caprae**

Ruwan Saeed Aljneibi Saeed Aljneibi

Follow this and additional works at: [https://scholarworks.uaeu.ac.ae/all\\_theses](https://scholarworks.uaeu.ac.ae/all_theses)



Part of the [Biotechnology Commons](#), and the [Molecular Biology Commons](#)

---

United Arab Emirates University

College of Science

Department of Biology

TRANSCRIPTOMIC ANALYSIS OF THE GLYCOPHYTIC CROP  
*Ipomoea aquatica* UNDER SALINITY CONDITIONS COMPARED  
TO ITS WILD HALOPHYTE RELATIVE *Ipomoea pes-caprae*

Ruwan Saeed Aljneibi

This thesis is submitted in partial fulfilment of the requirements for the degree of  
Master of Science in Molecular Biology and Biotechnology

Under the Supervision of Dr. Khaled Amiri

April 2021

### **Declaration of Original Work**

I, Ruwan Saeed Aljneibi, the undersigned, a graduate student at the United Arab Emirates University (UAEU), and the author of this thesis entitled “*Transcriptomic Analysis of the Glycophytic Crop Ipomoea aquatica Under Salinity Conditions Compared to its Wild Halophyte Relative Ipomoea pes-caprae*”, hereby, solemnly declare that this thesis is my own original research work that has been done and prepared by me under the supervision of Dr. Khaled Amiri, in the College of Science at UAEU. This work has not previously formed the basis for the award of any academic degree, diploma or a similar title at this or any other university. Any materials borrowed from other sources (whether published or unpublished) and relied upon or included in my thesis have been properly cited and acknowledged in accordance with appropriate academic conventions. I further declare that there is no potential conflict of interest with respect to the research, data collection, authorship, presentation and/or publication of this thesis.

Student’s Signature: *Ruwan Aljneibi*

Date: 14/4/2021

Copyright © 2021 Ruwan Saeed Aljneibi  
All Rights Reserved

## Approval of the Master Thesis

This Master Thesis is approved by the following Examining Committee Members:

- 1) Advisor (Committee Chair): Dr. Khaled Amiri

Title: Associate Professor

Department of Biology

College of Science

Signature



Date 22 April 2021

- 2) Member: Dr. Ranjit Vijayan

Title: Associate Professor

Department of Biology

College of Science

Signature



Date 22 April 2021

- 4) Member (External Examiner): Dr. Kourosch Salehi-Ashtiani

Title: Associate Professor

Center for Genomics and Systems Biology

Institution: New York University Abu Dhabi

Signature



Date April 22, 2021

This Master Thesis is accepted by:

Dean of the College of Science: Professor Maamar Benkraouda

Signature Maamar Benkraouda Date June 14, 2021

Dean of the College of Graduate Studies: Professor Ali Al-Marzouqi

Signature Ali Hassan Date June 14, 2021

Copy \_\_\_\_ of \_\_\_\_

## Abstract

This study focuses on the glycophytic crop *Ipomoea aquatica* (commonly known as water spinach) and its wild halophytic relative *Ipomoea pes-caprae*. *I. aquatica* is a crop with economic value; however, it is unable to tolerate high levels of salinity. Whereas its relative *Ipomoea pes-caprae* is able to grow and thrive in the harsh environment of the UAE. The main aim of this study is to analyze the genetic differences underlying the variation in the two plants' response to salinity and determine the genetic components that can be used to enhance *I. aquatica*'s tolerance to salinity. Accordingly, the plants were subjected to salinity stress for measuring physiological responses and the transcriptomes of the two plants were analyzed for mRNAs, miRNAs, and pathway enrichment. The analysis determined several crucial genetic differences between *I. aquatica* and *I. pes-caprae* during salinity stress. Many differences in the genetic responses were observed between these two plants, including the upregulation of High-affinity Potassium Transporter (HKT) in *I. pes-caprae* as well as the upregulation of a NAC3-like transcription factor. These differences can be used to genetically modify *I. aquatica* in order to enhance its salt tolerance levels.

**Keywords:** *Ipomoea aquatica*, *Ipomoea pes-caprae*, Bioinformatics analysis, Transcriptome analysis.

## Title and Abstract (in Arabic)

التحليل الشامل لجينات نبات السبانخ المائي ( *Ipomoea aquatica* ) و مقارنتها بجينات نبات ( *Ipomoea pes-caprae* ) من نفس الفصيلة لتحديد الجينات المتعلقة بتحمل الملوحة

### المخلص

تركز هذه الدراسة على نبات السبانخ المائي (*Ipomoea aquatica*) ونبات الحباية (*Ipomoea pes-caprae*) من نفس الفصيلة. نبات السبانخ المائي من النباتات ذات الأهمية الاقتصادية العالية إلا أنه غير قادر على تحمل الملوحة والمناخ الصعب في دولة الامارات، في حين ان نبات الحباية قادر على تحمل مستويات عالية من الملوحة مما يُمكنه من النمو والازدهار في البيئة القاسية لدولة الإمارات العربية المتحدة. الهدف الرئيسي من هذه الدراسة هو تحليل الاختلافات الجينية الكامنة وراء التباين في استجابة النباتين للملوحة وتحديد العوامل الجينية التي يمكن استخدامها لتعزيز تحمل السبانخ المائي للملوحة. وفقاً لذلك، تم تعريض النباتات لضغط الملوحة لقياس الاستجابات الفسيولوجية وتم تحليل العوامل الجينية ( mRNA, miRNA ) في كل من النباتين باستخدام النظم المعلوماتية. تمت إثر ذلك مقارنة الجينات بين النباتين، وتحديد الجينات التي تُمكن نبات الحباية من تحمل الملوحة. أدت الدراسة الى تحديد جينات عديدة، منها جين HKT وجين NAC3-like الذين يرتبطان بالتفاوت في قدرة النباتين على تحمل الملوحة. يمكن استخدام الجينات التي تم تحديدها في تجارب التعديل الوراثي لتعزيز مستويات تحمل الملح في نبات السبانخ المائي.

مفاهيم البحث الرئيسية: نبات السبانخ المائي، نبات الحباية، ، النظم المعلوماتية، التحليل الجيني.

## **Acknowledgements**

My thanks go to Dr. Khaled Amiri whose enthusiasm about bioinformatics helped to introduce me to this area of study. I am especially thankful to everyone at Khalifa Center for Genetic Engineering and Biotechnology for their immeasurable assistance during the course of this study, especially the Bioinformatics team (Dr. Kahled Hazzouri, Dr. Ling Li, Naganeeswaran Sudalaimuthuasari, Mariam AlZaabi, Fayas Purayil, and Jithin Balan).

I would like to thank my committee for their guidance, support, and assistance throughout my preparation of this thesis. I would like to thank the chair and all members of the Department of Biology at the United Arab Emirates University for assisting me all over my studies and research, especially Mr. Felix Labata. Special thanks go to my parents, husband, and family who supported me endlessly along the way.

## **Dedication**

*To my beloved parents, husband, and family*

## Table of Contents

Title .....	i
Declaration of Original Work .....	ii
Copyright .....	iii
Approval of the Master Thesis .....	iv
Abstract .....	vi
Title and Abstract (in Arabic) .....	vii
Acknowledgements .....	viii
Dedication .....	ix
Table of Contents .....	x
List of Tables.....	xii
List of Figures .....	xiii
List of Abbreviations.....	xiv
Chapter 1: Introduction .....	1
1.1 Overview .....	1
1.2 Statement of the Problem .....	1
1.3 Relevant Literature .....	2
Chapter 2: Methods .....	7
2.1 Experimental Design .....	7
2.1.1 Pilot Study .....	7
2.1.2 Salinity Stress Test and Sample Collection.....	8
2.2 RNA Extraction and Sequencing .....	9
2.3 Biochemical Analysis .....	10
2.3.1 Salt-stress Physiological Measurements .....	10
2.3.2 Analysis of Minerals .....	10
2.3.3 Analysis of Antioxidant Enzymes.....	11
2.4 Bioinformatics Analysis.....	12
2.4.1 Analysis of Transcriptome .....	12
2.4.2 Analysis of miRNA .....	14
2.4.3 Validation .....	15
Chapter 3: Results .....	17
3.1 Experimental Design.....	17
3.2 RNA Extraction and Sequencing .....	19
3.3 Biochemical Analysis .....	19
3.3.1 Salt-Stress Physiological Measurements.....	19
3.3.2 Analysis of Minerals .....	21

3.3.3 Analysis of Antioxidant Enzymes .....	23
3.4 Bioinformatics Analysis.....	25
3.4.1 Analysis of Transcriptome .....	25
3.4.2 Analysis of miRNA .....	39
3.4.3 Validation .....	41
Chapter 4: Discussion .....	43
4.1 HKT Gene .....	44
4.2 NAC3-like Gene .....	47
4.3 Photosynthesis Pathways .....	50
Chapter 5: Conclusion.....	52
5.1 Research Implications .....	52
References .....	54
Appendix .....	61

**List of Tables**

Table 1: Summary of the physiological response to salinity in relation to photosynthesis.....	51
--	----

## List of Figures

Figure 1: A Phylogenetic tree of seven <i>Ipomoea</i> species .....	2
Figure 2: Areas affected by soil salinity in the UAE .....	4
Figure 3: Cellular homeostasis .....	5
Figure 4: Salinity experiment design .....	8
Figure 5: Transcriptomics analysis pipeline .....	13
Figure 6: miRNA analysis pipeline.....	15
Figure 7: Chlorophyll measurements of both plants .....	17
Figure 8: Pilot study images.....	18
Figure 9: Physiological measurements.....	20
Figure 10: Analysis of minerals in <i>I. aquatica</i> and <i>I. pes-caprae</i> .....	22
Figure 11: Measurements of Hydrogen peroxide (H <sub>2</sub> O <sub>2</sub> ) and antioxidants (POD, SOD, and CAT) .....	24
Figure 12: PCA of samples .....	26
Figure 13: Differential gene expression analysis of Leaf samples from <i>I. aquatica</i> and <i>I. pes-caprae</i> .....	28
Figure 14: Differential gene expression analysis of Root samples from <i>I. aquatica</i> and <i>I. pes-caprae</i> .....	29
Figure 15: Differential expression of pathways <i>I. aquatica</i> leaves.....	32
Figure 16: Differential expression of pathways <i>I. aquatica</i> roots.....	33
Figure 17: Differential expression of pathways <i>I. pes-caprae</i> leaves.....	34
Figure 18: Differential expression of pathways <i>I. pes-caprae</i> roots.....	35
Figure 19: Differential gene expression of salt related identified pathways in Leaf samples.....	36
Figure 20: Differential gene expression of salt related identified pathways in Root samples .....	37
Figure 21: Venn Diagram showing all salt-related genes .....	38
Figure 22: Differentially expressed miRNAs in all samples .....	40
Figure 23: Log <sub>2</sub> fold changes detected with qRT-PCR.....	41
Figure 24: Regression analysis of <i>I. aquatica</i> (top) and <i>I. pes-caprae</i> (bottom) .....	42
Figure 25: Alignment of HKT protein sequence.....	45
Figure 26: Predicted interaction of miRNAs with HKT gene in <i>I. aquatica</i> and <i>I. pes-caprae</i> .....	46
Figure 27: Alignment of protein sequence of NAC3-like.....	48
Figure 28: Predicted interaction of miRNAs with NAC3-like gene in <i>I. aquatica</i> and <i>I. pes-caprae</i> .....	49

## List of Abbreviations

CTAB	Cetrimonium Bromide
ICP-OES	Inductively Coupled Plasma – Optical Emission Spectrometry
KEGG	Kyoto Encyclopedia of Genes of Genomes
miRNA	Micro Ribonucleic Acid
mRNA	Messenger Ribonucleic Acid
MS	Murashige and Skoog
Pfam	Protein Families Database
RNA	Ribonucleic Acid
SAM	Sequence Alignment Map

## Chapter 1: Introduction

### 1.1 Overview

Analysis of the glycophytic crop *Ipomoea aquatica* (*I. aquatica*), and its wild halophytic relative *Ipomoea pes-caprae* (*I. pes-caprae*), under salinity stress reveal several physiological and genetic differences that underly the plants' varying response to salinity. These genetic differences between the plants are examined in order to determine genes and pathways that can be used to enhance *I. aquatica*'s tolerance to salinity through genetic engineering. The transcriptomic analysis of the two plants reveals several candidate genes that can be used to enhance *I. aquatica*'s tolerance to salinity including High-Affinity Potassium Transporter (HKT) and the transcription factor NAC3-like gene.

### 1.2 Statement of the Problem

Salinity imposes a grand challenge to agriculture worldwide. *Ipomea aquatica* is a crop with economic value; however, its growth is hindered by its sensitivity to salt. In general, studies that aim to enhance the salinity tolerance of plants often focus on a single gene or pathway approach, which leads to limited outcome. A more thorough and focused approach is to study halophytic relatives of *I. aquatica* to understand the evolutionary divergence that resulted in speciation with marked phenotypic differences, namely, tolerance to salinity. This can lead to understanding the biological network that are involved in salt-tolerance, which can promote the development of salt-tolerant plant in a much more efficient manner.

### 1.3 Relevant Literature

The *Ipomoea* genus, in the Convolvulaceae family, comprises of 600-700 species; some of which are vegetable crops with great economic value like sweet potato and water spinach (Bai et al., 1969; Meira et al., 2012). Other plants in this genus are commonly used as ornamental flowers like *Ipomoea nil*, medicinal plants like *Ipomoea aquatica*, or items in religious rituals like *Ipomoea pes-caprae* (Meira et al., 2012).

One species of interest in the *Ipomoea* genus is *Ipomoea aquatica*, commonly known as water spinach. *I. aquatica* is a vegetable crop grown around the world, that has also been traditionally used as a medicinal plant for many ailments as far back as 200 B.C. (Austin, 2007; Meira et al., 2012; Shaikh, 2017). Although *I. aquatica* is a valuable crop, it is considered glycophytic and is not suitable for growing in arid and saline environment. As its' name suggests, *I. aquatica* is commonly grown in areas with access to water and low salinity. However, *I. aquatica* is related to some species of wild halophytic plants such as *Ipomoea pes-caprae* (Figure 1). The latter is a halophytic plant capable of growing in saline and arid environments including the UAE's costal region.

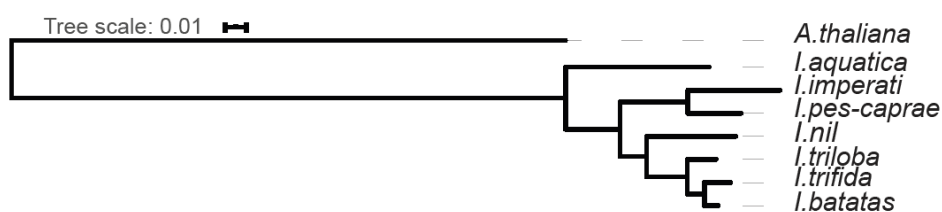


Figure 1: A Phylogenetic tree of seven *Ipomoea* species. The figure indicates the evolutionary relationship between these *Ipomoea* species. This phylogenetic tree was generated by aligning single-copy orthologues of *I. aquatica* and *I. pes-caprae* (identified through this study) to the same genes from other *Ipomoea* species (publicly available) and *Arabidopsis thaliana* (as an out-group).

*Ipomoea aquatica* and *Ipomoea pes-caprae* present a great opportunity to study the effects of salinity on halophytes versus glycophytes. Understanding the mechanisms underlying *I. pes-caprae*'s tolerance to salinity can present a way to enhance *I. aquatica* tolerance and ability to grow in environments similar to the UAE's.

Soil salinity is one of the main obstacles in growing *I. aquatica* in the UAE. This issue affects many regions around the world and hinders agricultural and economic development (Imadi et al., 2016; Shrivastava & Kumar, 2015). Worldwide, about 2000 ha of farmland are lost to salinization daily (Environment Agency - Abu Dhabi, 2019). This problem affects agricultural lands in the UAE and the wider Near East and North African region (Al Yamani & Athamneh, 2017). According to a soil study conducted by the Environmental Agency-Abu Dhabi on 4000 farms (2017), the rates of soil degradation in Abu Dhabi's irrigated land reached 85% (Al Yamani & Athamneh, 2017; Environment Agency - Abu Dhabi, 2019) (Figure 2). Soil salinization is considered one of the causes of soil degradation in the UAE; for example, about 90% of farmland in Al Ain was affected by soil salinity in 2017 (Al Yamani & Athamneh, 2017). The Environmental Agency-Abu Dhabi concluded that the major factors contributing to the UAE's soil salinity problem are salinization along the coastal areas due to seawater, inland inter-dunal salt intrusion areas (Sabkha), and irrigation with saline/brackish groundwater (Abdelfattah & Shahid, 2014; Al Yamani & Athamneh, 2017).

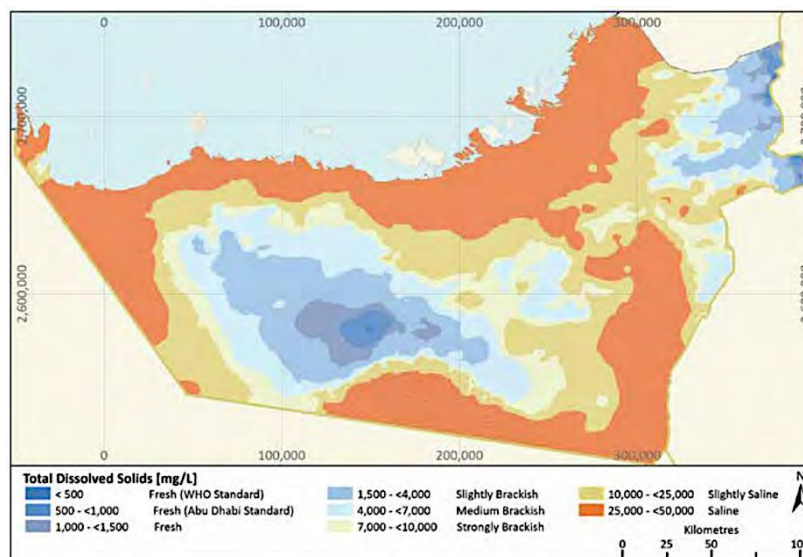


Figure 2: Areas affected by soil salinity in the UAE. This map indicated the extent of soil salinization all around Abu Dhabi as reported by the Environmental Agency-Abu Dhabi (Environment Agency - Abu Dhabi, 2019).

Salinity has a detrimental impact on plants in many ways including osmotic stress, ion toxicity, oxidative stress, and nutrient deficiency (Shrivastava & Kumar, 2015). To mitigate the effects of salinity, plants respond by using a myriad of diverging genetic pathways to closely regulate the cellular homeostasis and ensure its survival (Shrivastava & Kumar, 2015). Many genetic pathways like NHX, SOS, HKT were identified in relation to salinity stress response in plants (Mishra & Tanna, 2017). The regulation of salinity stress response in plants does not only involve protein-coding genes but also a score of microRNAs like miR156, miR169 and miR396 (Deng et al., 2015). These genes and microRNAs interact in a fine-tuned manner to regulate homeostasis inside the cell. Cellular homeostasis (stability in levels of ions) inside the cell have a direct impact on the survival of the plant (Hu & Schmidhalter, 2004). The salinity tolerance of many plants has been linked to their ability to compartmentalize or extrude ions (Flowers & Colmer, 2008; Hu & Schmidhalter, 2004) (Figure 3).

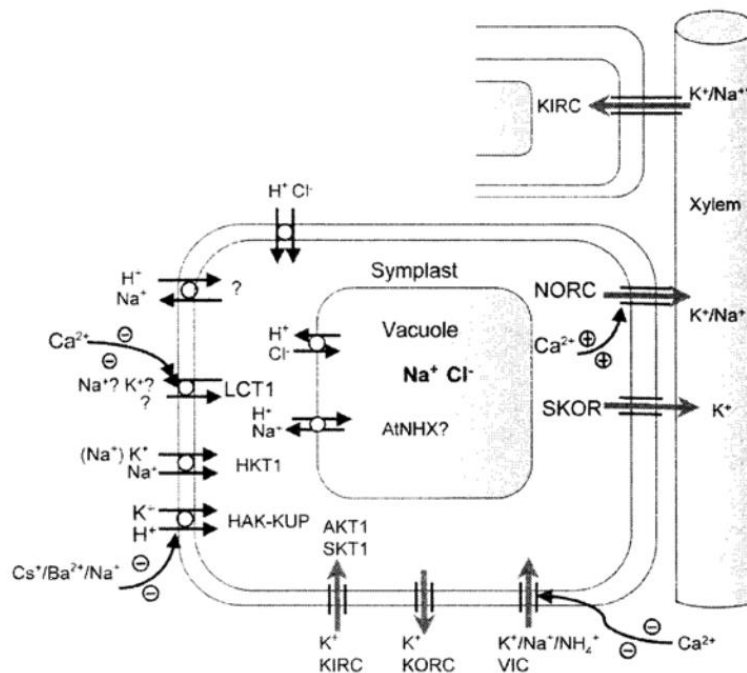


Figure 3: Cellular homeostasis. The diagram shows channels and transporters that control the influx, efflux, translocation, and compartmentalization of ions in plant cells (Hu & Schmidhalter, 2004).

Plants that are capable of withstanding higher levels of salinity (halophytes) represent a genetic resource for improving crops that are most affected by salinity (glycophytes). Understanding the transcriptome of halophytes and glycophytes is a crucial step in developing crops that are more resilient to salinity stress. Many studies have been conducted to understand the genetic aspects of salt-tolerance. In recent years, with the development of Next Generation Sequencing (NGS), transcriptomics studies have been at the forefront of plant salt-tolerance studies. Attempts to analyze the expression of genes under salinity stress in many plants resulted in a deeper understand of the genetic mechanisms that govern tolerance. For example, studies on rice varieties that exhibit tolerance to salinity, compared to sensitive varieties, have successfully identified genes and pathways that can be used in genetic engineering studies (Baldoni et al., 2016; Wang et al., 2018).

Similar research approaches were used to study miRNA expression in many plant species like switchgrass (Xie et al., 2014).

Transcriptomics analysis studies can shed a new light on the differences in salinity tolerance among *Ipomoea* species. Transcriptomics studies have been performed on few *Ipomoea* species previously. Recent transcriptomics studies conducted on *I. aquatica* successfully found cultivar-specific mechanisms for cadmium accumulation in roots including genes and miRNAs (Huang et al., 2016; Shen et al., 2017). A recently published transcriptomics study on *I. pes-caprae* under salinity suggested some genes that can be used to enhance the salt-tolerance of sweet potato (*Ipomoea batatas*) (Liu et al., 2020).

In this study, a deep analysis of the transcriptome and microRNA expression under salinity conditions is conducted for both *I. aquatica* and its halophytic wild relative *I. pes-caprae*. The results of this analysis can be used to genetically engineer *I. aquatica* to increase its ability to tolerate salinity.

## Chapter 2: Methods

### 2.1 Experimental Design

#### 2.1.1 Pilot Study

A pilot test was first conducted to determine the appropriate concentration of sodium chloride (NaCl) to induce salinity-stress in the plants in hydroponic growth chambers for a prolonged period of time without causing plant death. The chlorophyll content in both plants' leaves was measured as a marker for the plants ability to withstand salinity stress. It has been reported that during high level stress the chlorophyll content in plants will drop (Agathokleous et al., 2020); however, halophytes are able to regulate the levels of chlorophyll in their leaves (Redondo-Gómez et al., 2010). Seeds of *I. aquatica* were germinated on damp filter paper in dark conditions at 25°C for five days. The seedlings were then transported to hydroponic chambers containing Murashige and Skoog (1/10 MS-pH 6) liquid growth medium under growth lights and allowed to grow for two weeks; then the plants were divided into hydroponic chambers containing 1/10 MS-pH 6 growth solution with increasing concentrations of NaCl (0, 100, 150, 200, 250, 300 mM). The plants were then closely monitored over the course of one week to determine the phenotypic effects of salinity on leaves and roots. The chlorophyll content of the leaves was determined using Chlorophyll Meter SPAD-502Plus machine. To test *I. pes-caprae* tolerance levels to salinity, young shoot cuttings from an established *I. pes-caprae* plant available at KCGEB were collected and grown in hydroponic chambers containing 1/10 MS-pH 6 solution until roots were established. After two weeks of growth, the plants were divided into six chambers with increasing NaCl concentration as done for *I. aquatica*.

### 2.1.2 Salinity Stress Test and Sample Collection

*I. aquatica* plants were germinated and grown for two weeks as in the pilot experiment. After two weeks of growth, *I. aquatica* plants were divided into three hydroponic chambers: one chamber containing (1/10 MS-pH 6), and two chambers containing (1/10 MS-pH 6 + 100 mM NaCl). Triplicates of both leaf and root samples were collected from each chamber at 4 hrs, 24 hrs, 3 days, and 7 days, and flash-frozen in liquid nitrogen and stored at -80°C. Samples grown in MS alone were labeled as control, while sample grown in MS+NaCl were labeled as salt-treated. Samples collected from 4 hrs and 24 hrs were considered as Early phase, while samples from 3 and 7 days were considered as Late phase (Figure 4). *I. pes-caprae* plants were grown from cuttings as in the pilot study then placed into three hydroponic chambers: one chamber containing (1/10 MS-pH 6), and two chambers containing (1/10 MS-pH 6 + 200 mM NaCl). Samples from *I. pes-caprae* leaves and root were collected, stored, and labeled in the same manner as *I. aquatica*.

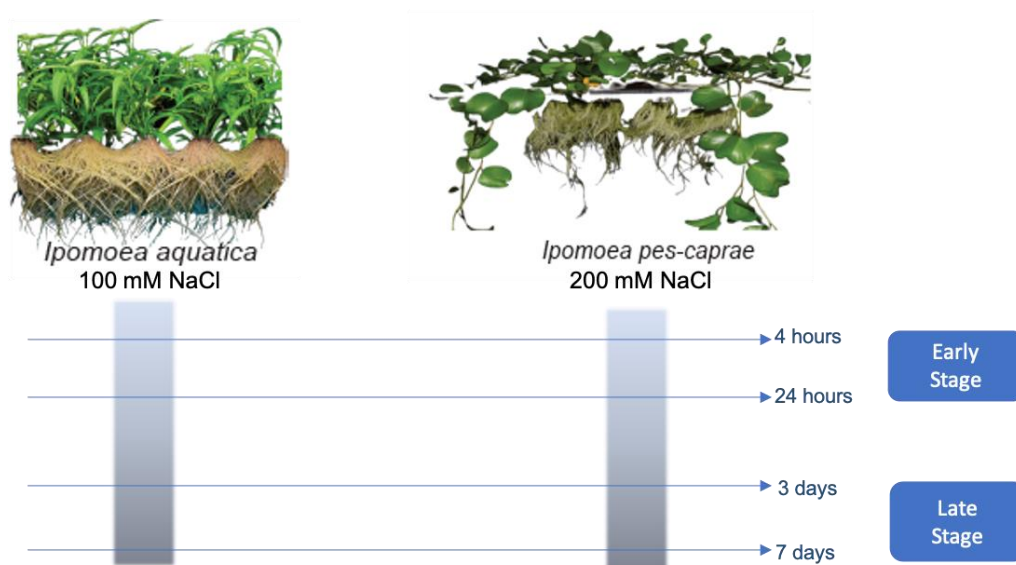


Figure 4: Salinity experiment design. This figure shows the NaCl concentrations used as well as the time points for sample collection.

## 2.2 RNA Extraction and Sequencing

Samples collected during the experiment were used in total RNA extraction. The RNA from each sample was sequenced and used for downstream bioinformatics analysis. The leaf and root samples of both plants were homogenized with liquid nitrogen, then RNA was extracted using extraction buffer containing CTAB + 2%  $\beta$ -mercaptoethanol, followed by chloroform:isoamylalcohol (24:1) wash and 70% Ethanol precipitation. The quality of the RNA was determined using Nanodrop machine followed by 1% agarose gel electrophoresis.

For the salt-treated samples of both plants, high-quality equal amounts of RNA were combined from 4 hrs and 24 hrs sample to produce the “Early” triplicate samples of leaf and root, while RNA from 3 and 7 days was combined to produce “Late” triplicate samples for leaf and root (as shown previously in Figure 4).

A total of 36 RNA samples were sent to Macrogen Inc. (South Korea) for sequencing. To sequence the total RNA, library preparation was constructed with TruSeq Stranded Total RNA LT Sample Prep Kit (Plant) according to Macrogen’s Total RNA LT Sample Prep Guide (Part # 15031048 Rev. E). The library was then used in paired-end sequencing on Illumina platform (read length 101bp). To sequence miRNA, high-quality RNA samples were used to construct a sequencing library using TruSeq small RNA Library Prep Kit according to Macrogen’s TruSeq small RNA Library Prep Guide (Part # 15004197 Rev. G). The library was then used in single-end sequencing on Illumina platform (read length 51bp).

## **2.3 Biochemical Analysis**

### **2.3.1 Salt-stress Physiological Measurements**

The physiological changes in the plants under salinity stress were closely monitored. These include the measurements of photosynthesis and water-loss rate. These physiological responses are a clear indication of the plants' response to salinity; understanding the differences between the two plants physiologies under salinity is crucial. Halophytic plants are able to maintain more stable levels of photosynthesis during stress while reducing water loss via reducing transpiration rate (Liu et al., 2011; Yang et al., 2020). Physiological measurements of the plants were recorded using Licor 6800 (LI-COR Biosciences, 2020). Gas Exchange and Fluorescence System with ambient CO<sub>2</sub> concentration set to 400  $\mu\text{molmol}^{-1}$ . The measurements were made in triplicates for control and treated leaf samples for both plants. The measurements recorded by Licor include leaf transpiration rate, intercellular CO<sub>2</sub> concentration, CO<sub>2</sub> assimilation rate, and stomatal conductance. The instantaneous carboxylation efficiency was calculated from the intercellular CO<sub>2</sub> concentration and CO<sub>2</sub> assimilation rate measurements (Dias et al., 2017). These measurements were important to understand how both plants respond to stress physiologically.

### **2.3.2 Analysis of Minerals**

During Salinity stress, halophytic plants have been shown to maintain better ion homeostasis in their tissue. For this reason, measurements of the concentration of several minerals (Na<sup>+</sup>, Cl<sup>-</sup>, K<sup>+</sup>, Ca<sup>2+</sup>, Mg<sup>2+</sup>) in both leaf and root samples of both plants were performed using Inductively Coupled Plasma Optical Emission spectroscopy (ICP-OES).

Homogenized plant tissue was treated with acids to remove organic matter and solubilize the minerals. The solution was then passed through a nebulizer to produce an aerosol, which was then excited using plasma torch. The element-specific emission spectra were then detected using Varian ICP-OES model 710-ES machine, and the concentration of each element was determined. All ICP-OES measurements were conducted in College of Science, Department of Animal Nutrition Laboratory, United Arab Emirates University, UAE according to their guidelines.

### **2.3.3 Analysis of Antioxidant Enzymes**

Salinity stress can induce accumulation of Reactive Oxygen Species (ROS) in plant tissue, which causes oxidative damage and hinder the survival of the plants (Tanveer & Ahmed, 2020). To alleviate the damage, plants produce antioxidant enzymes that remove reactive oxygen species from the cell. These enzymes include Peroxidase (POD), Catalase (CAT), and Superoxide Dismutase (SOD) (Dias et al., 2017; Hossain & Dietz, 2016). Plant enzymes were extracted from homogenized samples using a Potassium Phosphate buffers (Monnet-Tschudi et al., 2006; Samantary, 2002). Peroxidase assay was conducted according to (Arnnok et al., 2010). Catalase and Superoxide dismutase assays were conducted according to (Cakmak & Marschner, 1992; Monnet-Tschudi et al., 2006) and the calculations of CAT activity were done using equations from (Tijssen, 1985). All measurements were carried out using Evolution™ 201/220 UV-Visible Spectrophotometers. Hydrogen peroxide levels were measured according to (Sergiev et al., 1997).

## **2.4 Bioinformatics Analysis**

### **2.4.1 Analysis of Transcriptome**

The total mRNA of both species was analyzed in order to identify genes or pathways that are enriched during salinity stress. Deciphering differences in the pathways enriched in both plants under salinity conditions can lead to identifying the underlying genetic differences that led to their contrasting abilities to tolerate salinity. The analysis pipeline is described in Figure 5. Briefly, The FASTQ files generated from Illumina sequencing were used to analyze the transcriptome of leaf and root samples from both plants. Sequences were trimmed to remove adapter sequences and low-quality sequences using Trimmomatic program (Bolger et al., 2014). The trimmed sequences were read-mapped to the genome using HISAT2 alignment program to produce BAM files for each sample (Kim et al., 2019 ; Li et al., 2009). The BAM files were then assembled using StringTie2 program into a non-redundant list of all genes (Kovaka et al., 2019); the assembled reads were then merged for each of leaf and root samples and the transcriptomic data were reassembled according to the StringTie2 user manual to obtain read coverage tables in gtf format (Kovaka et al., 2019; JHU, 2020). The gtf files were converted to FASTA format using Gffread program (Pertea & Pertea, 2020). A python3 script was used to obtain read count tables of genes and transcripts (JHU, 2020). the count tables generated were then used to analyze the differentially expressed genes in all samples by DESeq2 program using q-value 0.05 (Love et al., 2020; Love et al., 2014). The results were sorted into three categories (Upregulated, Neutral, Downregulated) and Venny tools was used to visualize commonly upregulated and downregulated genes between early and late samples (Oliveros, 2020).

Functional annotation of the transcriptome data was generated by using DIAMOND to align sequences to protein database from Uniprot/EMBL-EBI to identify protein families (pfam) for each gene (Buchfink et al., 2015). Further functional annotation was achieved using KEGG-KAAS analysis tool to generate KEGG Orthology (KO) assignment for the genes in the transcriptome data (Moriya et al., 2007). This tool was used to determine the pathways involved in the transcriptome. Gene Ontology analysis was obtained using dcGO Enrichment online tool to determine the enriched pathways using pfam list of the differentially expressed results (Fang & Gough, 2013). This tool identifies Gene Ontology term (GO) and sort then into three sub-ontologies: biological process, cellular component, and molecular function. The sequences were also mapped against *Arabidopsis thaliana* database to match the Ipomoea genes to genes found in *A. thaliana*. This was prepared to facilitate the comparison between the transcriptomes of the two plants.

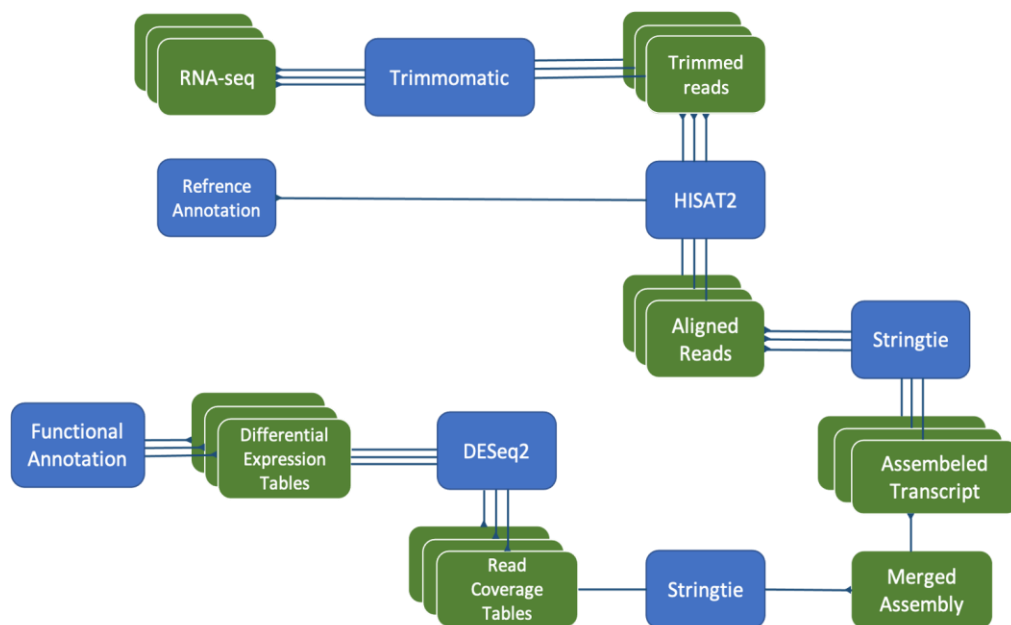


Figure 5: Transcriptomics analysis pipeline. This diagram shows the programs used in each step of the transcriptome analysis.

### 2.4.2 Analysis of miRNA

Non-coding RNAs have been shown to have important regulatory roles in gene expression. For this reason, the analysis of miRNAs enrichment in both plants during salinity stress was important. The miRNA analysis pipeline is described in Figure 6. The analysis of miRNA in all leaf and root samples of both plants was assessed using sequences generated by Macrogen Inc. (South Korea) Illumina sequencing. The quality of the sequences was determined using FastQC tool. Since miRNAs are in average 22 bp (O'Brien et al., 2018) and the sequence generated by Illumina is 51 bp in length, sequences containing the adapter were most likely to be miRNA. The UEA sRNA Workbench was used to remove sequences that did not contain any adapters as well as r/tRNA sequences, then trim the filtered sequences to remove the adapters (Stocks et al., 2018). Valid reads were determined to be between 16bp and 35bp in length. To identify known miRNAs from the trimmed sequences, miRBase was used to obtain all known miRNA sequences and makeblastdb program was then used to create a local miRBase database for miRNA (Altschul et al., 1990; Kozomara et al., 2019). The trimmed reads were then aligned to the miRBase local database using BlastN tool while allowing 2 mismatches maximum to determine known miRNA present in the samples (Altschul et al., 1990). Sequences that did not match any known miRNAs were used to identify any novel miRNAs using mireap program (Qibin, 2020). The count data generated from the previous programs were utilized to determine differentially expressed miRNAs in the samples using DESeq2 (Love et al., 2014). To identify the targets of miRNA present in the sample, both miRanda and psRNATarget programs were used (Betel et al., 2010; Dai et al., 2018; Quillet et al.,

2020). The predicted targets were then sorted based on energy value ( $<-25$ ) and expectation value (lowest) to determine the most significant targets.

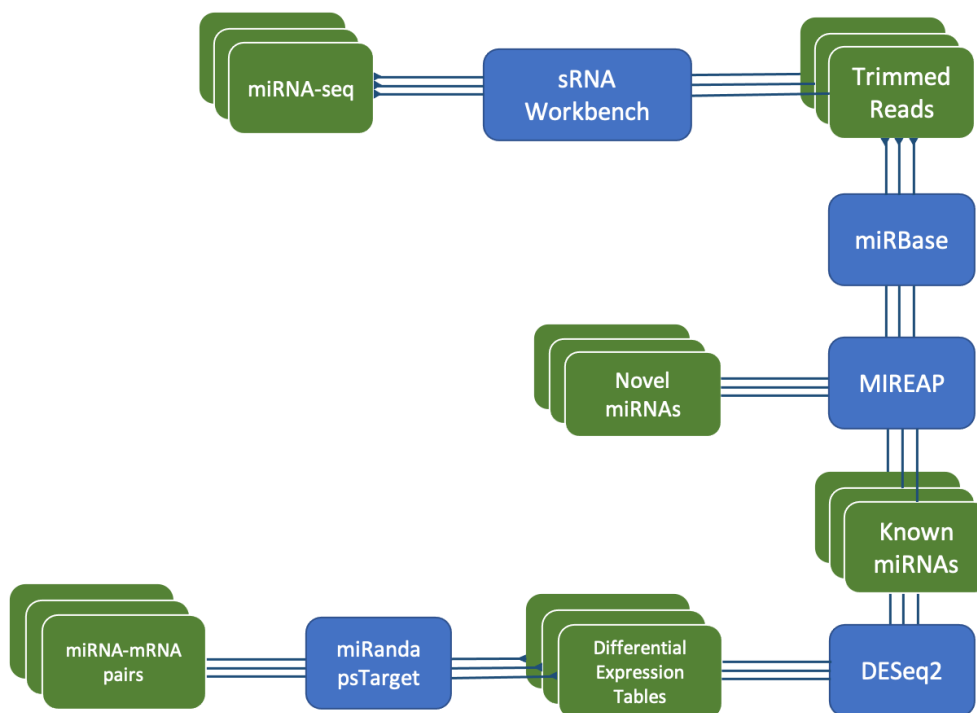


Figure 6: miRNA analysis pipeline. This diagram shows the programs used in each step of miRNA analysis.

### 2.4.3 Validation

Differentially Expressed Genes (DEGs) were analyzed to determine salt-tolerance related genes in both *I. aquatica* and *I. pes-caprae*. The expression level of 10 candidate salt-related genes were validated using Reverse transcription PCR followed by quantitative real time PCR (qRT-PCR). RNA was extracted from *I. aquatica* and *I. pes-caprae* samples (leaf and root at 0 hrs, 4 hrs, 24 hrs, 3 days, and 7 days) using Maxwell® RSC Plant RNA kit and Maxwell RSC48 machine (Promega). First strand cDNA was synthesized from 1 mg of RNA using the Quantitect® Reverse Transcription kit (Qiagen) according to the manufacturer's instructions. Then, the

qPCR reaction was done using diluted cDNA (1:3) and Fast™ SYBR Green (Applied Biosystems) as per the manufacturer instructions, and threshold cycle (Ct) was determined using StepOnePlus Real-Time PCR system (Applied Biosystems). Each reaction was done using three biological replicates and two technical replicates and the Ct was averaged for each gene. The average  $\Delta\Delta C_t$  was used to determine the fold change of candidate genes in salt-treated samples relative to control samples, both normalized against endogenous reference gene (Actin/ELF) (Rao et al., 2013). The reference genes were chosen by looking at genes with stable expression in control and treated samples over all stages.

Differentially expressed miRNA were to be validated using stem-loop qPCR. RNA was extracted using mirVana™ miRNA Isolation Kit (Invitrogen). Stem-loop primers were designed according to (Chen et al., 2005) and used to synthesize cDNA using Quantitect® Reverse Transcription kit (Qiagen). Forward and reverse primers were to be used for qPCR using PowerUp™ SYBR Green (Applied Biosystems) as per the manufacturer instructions.

## Chapter 3: Results

### 3.1 Experimental Design

The Pilot study conducted on *I. aquatica* revealed that, in hydroponic chambers, the chlorophyll content of leaves decreased considerably with the increase of NaCl concentrations as well as the duration of salt stress (Figure 7); whereas, *I. pes-caprae* leaves showed only a slight reduction in chlorophyll content over the course of the experiment. This is a strong indication of *I. pes-caprae*'s ability to maintain cellular homeostasis during stress. Studies have shown that, during stress, accumulation of reactive oxygen species hinders the plant's ability to maintain its chlorophyll levels (Agathokleous et al., 2020). As the results indicate, *I. aquatica* was not able regulate its cellular homeostasis and sustained a more severe decrease in chlorophyll levels.

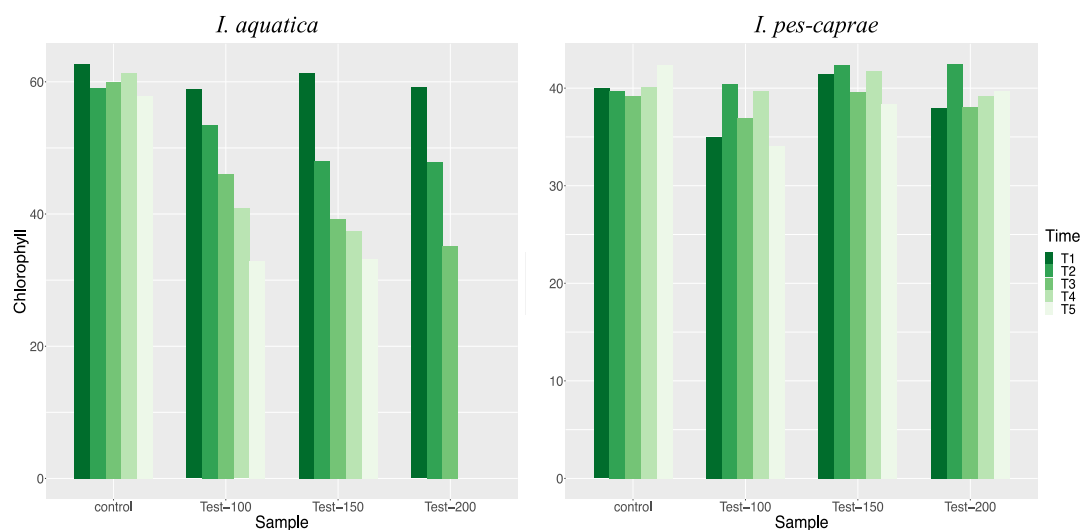


Figure 7: Chlorophyll measurements of both plants. Plants were subjected to multiple concentrations of NaCl (0, 100, 150, 200 mM NaCl) and the chlorophyll levels were measured at 5 timepoints T1-5 (0 hrs, 4 hrs, 24 hrs, 3 days, 7 days respectively). Chlorophyll levels in *I. aquatica* at 200 mM NaCl on day 7 was not possible due to extreme wilting of the leaves.

As shown in the images captured during the pilot study, *I. aquatica* showed wilting at 100 mM NaCl after one day with clear yellowing of older leaves, but by the end of the experiment the wilting of older leaves was accompanied by growth of new leaves. This was determined to be a part of the plant's response and adaptation to salinity. In 200 mM NaCl, *I. aquatica* showed wilting of leaves from the first few hours and by the fourth day the plants were completely wilted. The pilot study conducted for *I. pes-caprae* showed that at 200 mM NaCl, the leaves showed some yellowing after 24 hours, but they were able to grow new leaves after 7 days (Figure 8). This phenotype was similar to that exhibited by *I. aquatica* under 100 mM NaCl for 7 days. Given the observed phenotypes and chlorophyll measurements of the plants in the pilot test, it was determined that *I. aquatica* can be grown in 100 mM NaCl hydroponic conditions for 7 days, while *I. pes-caprae* is able to tolerate higher concentration of 200 mM NaCl for the same period of time. The salt-stress experiment was conducted, and samples were collected for analysis as described in the Methods section.

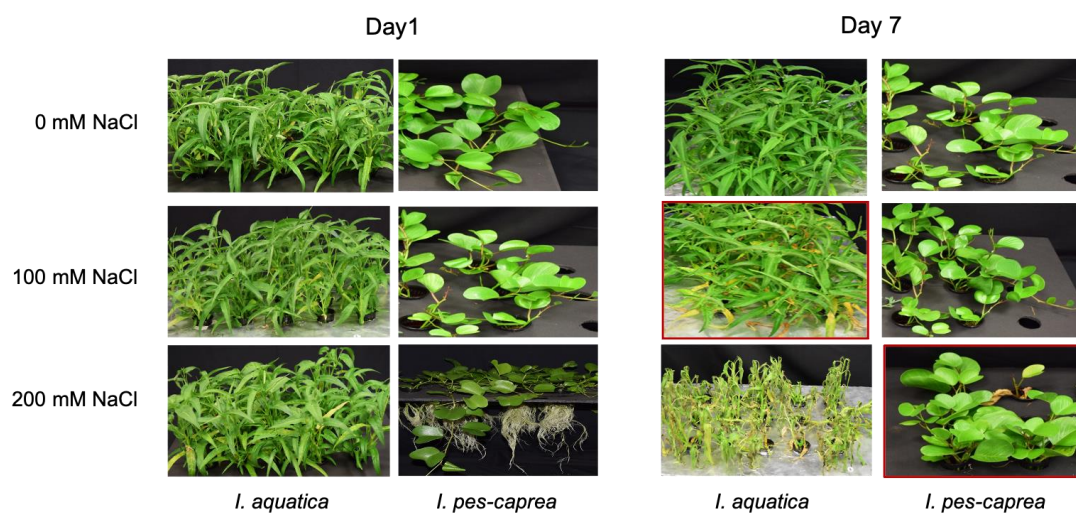


Figure 8: Pilot study images. The figure shows the plants after 7 days of salt treatment in 0, 100, and 200 mM NaCl.

### 3.2 RNA Extraction and Sequencing

The integrity of all RNA extracted was determined using Nanodrop® spectrophotometer and agarose gel electrophoresis. Final RNA quality testing at Macrogen using Agilent 2100 Bioanalyzer system determined that all samples were high in quality when received and were acceptable for sequencing. The quality control analysis of both Next Generation Sequencing (NGS) Library as well as the RNA sequencing with Illumina revealed that all sequenced were good in quality and acceptable for sequencing.

### 3.3 Biochemical Analysis

#### 3.3.1 Salt-Stress Physiological Measurements

Physiological measurements detected during salinity stress show that *I. aquatica* was not able to maintain its photosynthesis rates under salinity, and it was experiencing a higher rate of water loss through stomatal conductance. However, *I. pes-caprae* was able to keep water loss to a minimum under the crucial early stages of salinity stress. It was also capable of keeping its photosynthesis rate at a much more stable level than *I. aquatica*.

The results shown in Figure 9 indicates that during salinity stress, *I. aquatica* photosynthetic rate decreases gradually over time. Moreover, the transpiration rate in the leaves as well as the stomatal conductance to H<sub>2</sub>O increases over time. The intracellular carbon dioxide concentration did not change during the first 24 hours, but then increased in the 3- and 7-day measurements (Figure 9). In the case of *I. pes-caprae*, all measurements regarding the photosynthesis rate, transpiration rate, and stomatal conductance to H<sub>2</sub>O indicate a dramatic decrease within the first 24 hours

followed by slight recovery afterwards. The intracellular carbon dioxide concentration spikes after 4 hours then gradually decrease at 24 hours before it plateaued (Figure 9). The photosynthesis rate and intracellular carbon dioxide concentration were used to calculate the rate of instantaneous carboxylation ( $A/C_i$ ) (Figure 9). In *I. aquatica*, instantaneous carboxylation decreased considerably over the entire course of the experiment. However, *I. pes-caprae* showed a dramatic decrease during the early stage (4-24 hours) followed by an increase in the late stage (3-7 days).

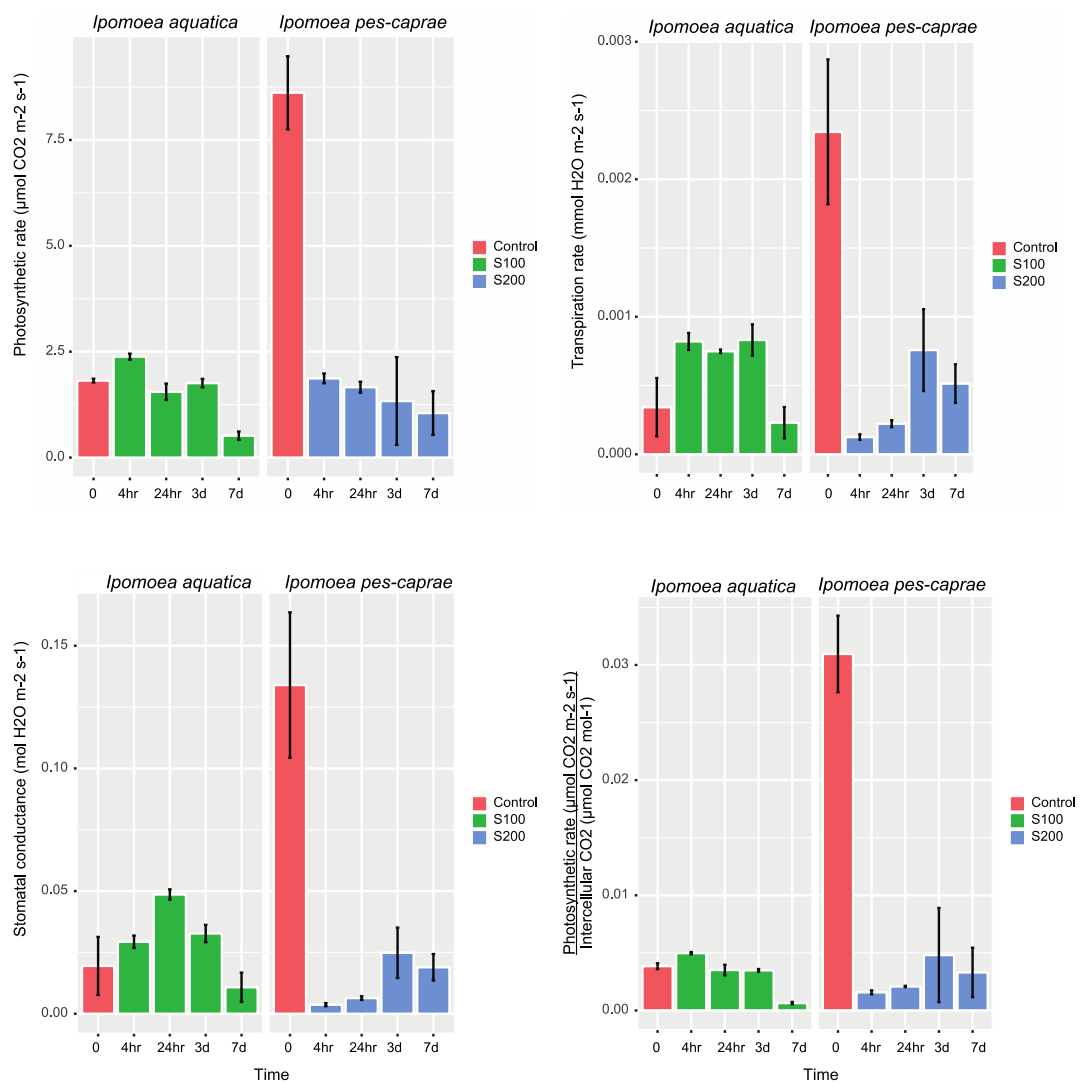


Figure 9: Physiological measurements. Data was collected from both plants including the photosynthesis rate, transpiration, stomatal conductance rates, as well as instantaneous carboxylation rate.

### 3.3.2 Analysis of Minerals

The results of mineral analysis indicate that *I. pes-caprae* is capable of maintaining homeostasis by efficiently regulating the ratios of mineral accumulation in the plant roots. On the other hand, *I. aquatica* was not able to maintain homeostasis in the roots. All measurements of mineral content can be found in (Appendix Table 1; Figure 10). The results of the analysis revealed that calcium ( $\text{Ca}^{2+}$ ) content in *I. aquatica* leaves did not change significantly throughout the experiment; however, it continually decreased in *I. pes-caprae*. In the roots, the calcium content decreased in the early stage then slightly increased in the late stage for both plants. The magnesium ( $\text{Mg}^{2+}$ ) content in leaves of both plants did not change significantly; however, it gradually decreased in the roots on *I. aquatica* but not in *I. pes-caprae*. The ratios of sodium ( $\text{Na}^+$ ) and potassium ( $\text{K}^+$ ) were measured to calculate the  $\text{Na}^+/\text{K}^+$  ratio. This ratio indicates the plant's ability to tolerate salinity. This ratio was higher in *I. pes-caprae* roots than in *I. aquatica* roots; however, in the leaves it was similar in both plants over the course of the experiment. The chloride ( $\text{Cl}^-$ ) content was measured and revealed the rate of Chloride accumulation was similar in the leaves of both plants. However, *I. pes-caprae* roots were able to retain significantly more chloride than *I. aquatica* roots.

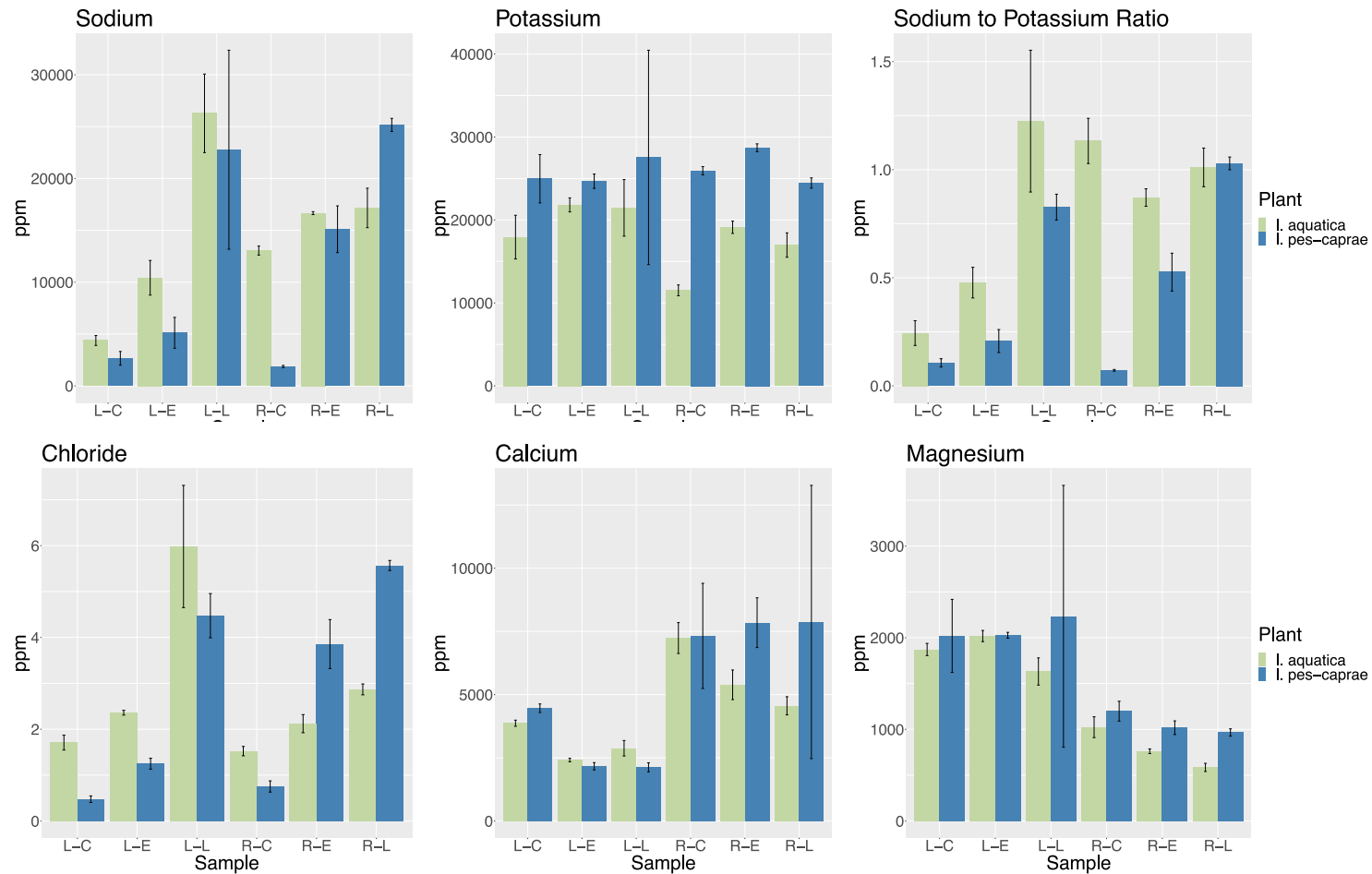


Figure 10: Analysis of minerals in *I. aquatica* and *I. pes-caprae*. The figures indicate the concentrations of minerals measured in both plants' Leaf (L) and Root (R) tissues in the Control (C), Early (E) and Late (L) samples. All concentrations are expressed as parts per million (ppm).

### 3.3.3 Analysis of Antioxidant Enzymes

The levels of  $H_2O_2$  as well as the three antioxidant enzymes (POD, CAT, SOD) was measured in both plants' leaves and roots (Figure 11). The results indicated that in *I. aquatica*, the concentration of  $H_2O_2$  in leaves and roots behaves oppositely from each other over the course of the experiment. The concentration of  $H_2O_2$  decreased in the leaves in the early stage then increased slightly. This can be attributed to the changes in concentration of the antioxidant enzymes. Indeed, in the leaves, the concentration of POD and CAT increase slightly in the early stages corresponding to the decrease in  $H_2O_2$ . In *I. aquatica* roots, the concentration of  $H_2O_2$  increased in the early stage then decreased slightly which corresponds to the changes in the concentration of CAT and SOD. On the other hand, *I. pes-caprae* was able to reduce the concentration of  $H_2O_2$  in both the leaves and roots over the course of the experiment (Figure 11). In the leaves, the reduction of  $H_2O_2$  may correspond to the increase in POD content. In the roots, the reduction in  $H_2O_2$  may correspond to the increase in SOD and CAT.

It is evident that the changes in  $H_2O_2$  concentration were more profound in *I. pes-caprae* leaves than *I. aquatica*. However, the concentration in the roots of both plants paint a different story. *I. pes-caprae* was able to reduce  $H_2O_2$  concentration throughout the experiment, while *I. aquatica* showed an extreme increase in  $H_2O_2$  concentration followed by a slight decrease. This may indicate that an aspect of *I. pes-caprae*'s halophytic traits is its ability to better maintain lower concentrations of reactive oxygen species in both leaves and roots.

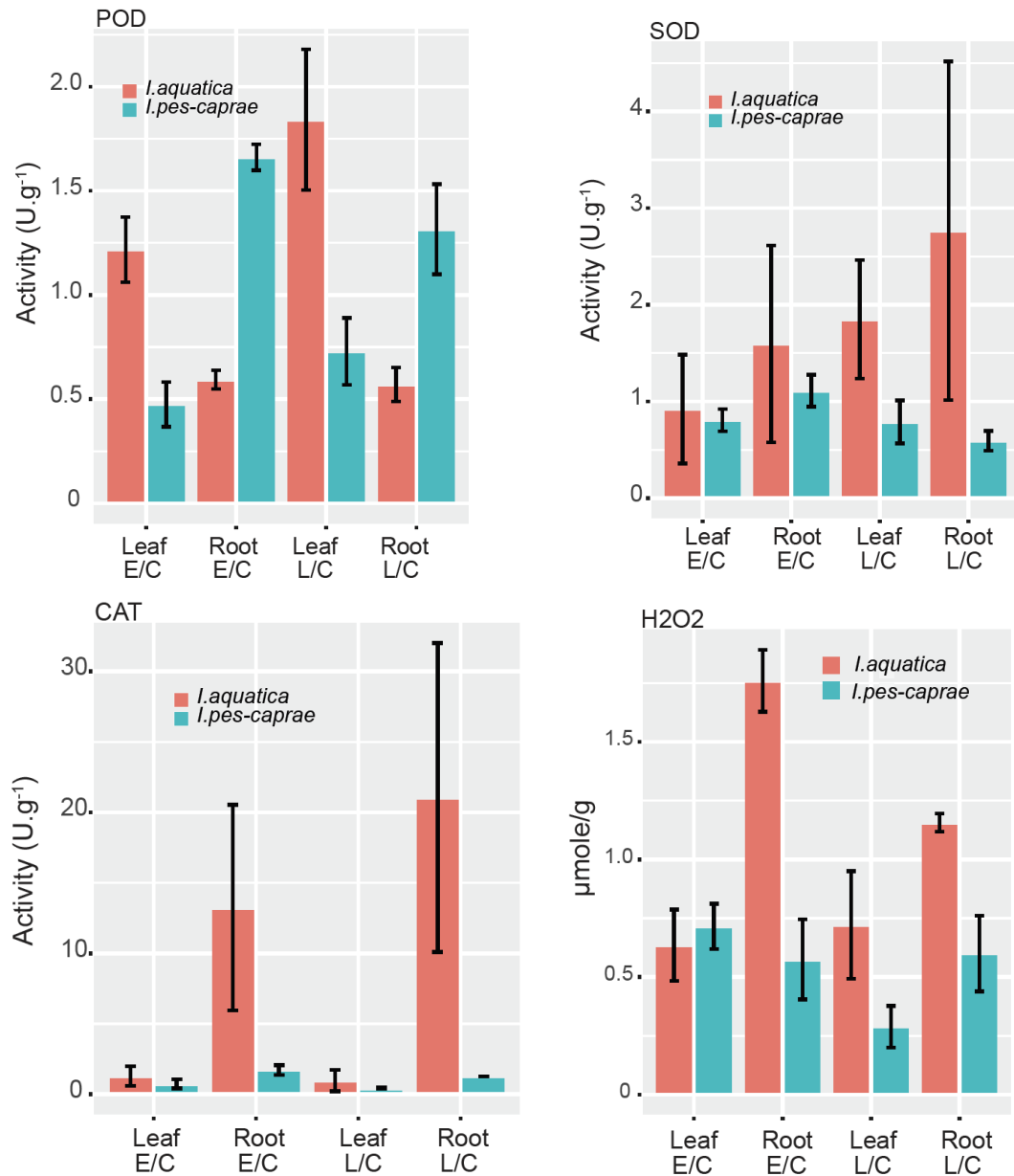


Figure 11: Measurements of Hydrogen peroxide ( $\text{H}_2\text{O}_2$ ) and antioxidants (POD, SOD, and CAT). The bars show the measured activity in Control versus Early sample (E/C) and Control versus Late sample (L/C) for both leaves and roots.

### 3.4 Bioinformatics Analysis

#### 3.4.1 Analysis of Transcriptome

The sequence quality was assessed by FastQC indicates that all samples had high quality sequences and very few needed to be trimmed (Appendix Figure 1). The percentage of reads remained after adapter trimming with Trimmomatic was high for all samples (Appendix Tables 2 and 3). Using HISAT2, the alignment for *I. aquatica* and *I. pes-caprae* was reported for all samples (Appendix Tables 2 and 3). The alignment of *I. aquatica* leaf samples were between 97.70% and 95.87%, while root samples were between 90.95% and 87.57% (Appendix Tables 2 and 3). For *I. pes-caprae*, the alignment of leaf samples was between 97.23% and 95.61%, and for root samples between 90.95% and 87.57% (Appendix Tables 2 and 3). The total number of assembled reads for leaves and roots of both plants is shown in (Appendix Tables 2 and 3). The Principal Component Analysis (PCA) is shown in Figure 12. PCA is often used as a sample-level quality control tool. Each dot in the PCA figure represents a sample and its transcription profile, so samples with similar gene transcription profile cluster closer to each other. The results of the PCA indicate that all samples clustered well together and downstream differential expression analysis can be done.

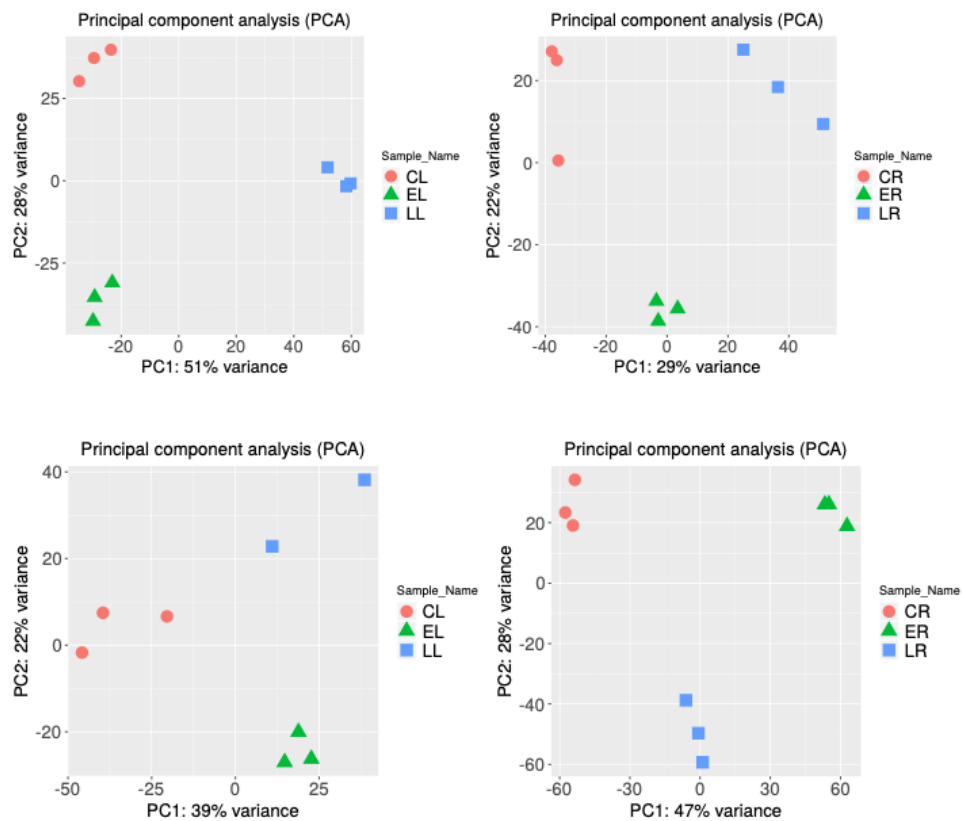


Figure 12: PCA of samples. *I. aquatica* leaves (top left), and roots (top right). *I. pes-caprae* leaves (bottom left), and roots (bottom right).

Differential gene analysis using DESeq2 results as well as analysis of the enriched pathways are shown in the Figures below. Figure 13 shows the numbers of up- and downregulated genes in *I. aquatica* and *I. pes-caprae* leaf samples and Figure 14 represents the differentially expressed genes for the root samples, in all stages of the experiment. The differential expression analysis of genes was achieved by three pairs of comparisons: Early and Control samples, Late and Control samples, as well as Late and Early samples. Genes from the Early and Late samples were compared to Control to identify the absolute differential expression in these samples. Then, the Late and Early samples were compared to study the expression profiles of genes throughout the experiment.

For example, a Bet-domain containing protein (pfam: PF00407) was found to be differentially expressed in the leaves of *I. aquatica*. This gene downregulated 7 folds in the Early samples, but the expression was found to be neutral in the Late sample (0.8 fold change). When comparing the Late to Early samples, the fold change of this gene is determined to be upregulated by 8.5 folds. Thus, looking at the differential expression of genes in all three pairs of comparisons gives a more comprehensive understanding of the expression profile of a gene.

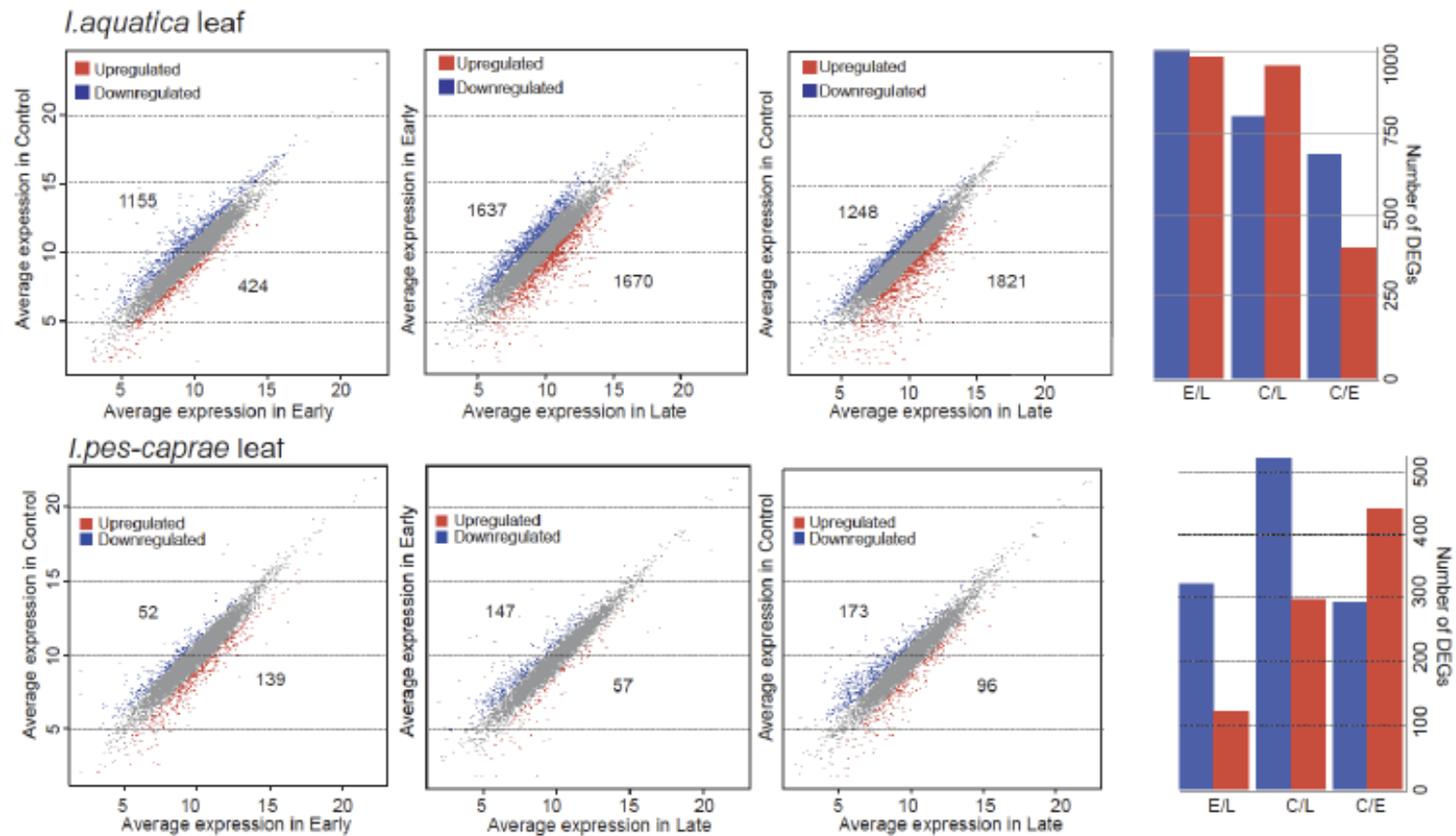


Figure 13: Differential gene expression analysis of Leaf samples from *I. aquatica* and *I. pes-caprae*. The figures show the numbers of differentially expressed genes in the Leaf in Early and Late samples compared to the Control samples, as well as Late sample compared to Early sample. The scatter plots on the left represent all genes, and the bar graphs on the right represent the number of genes up- and downregulated in each sample.

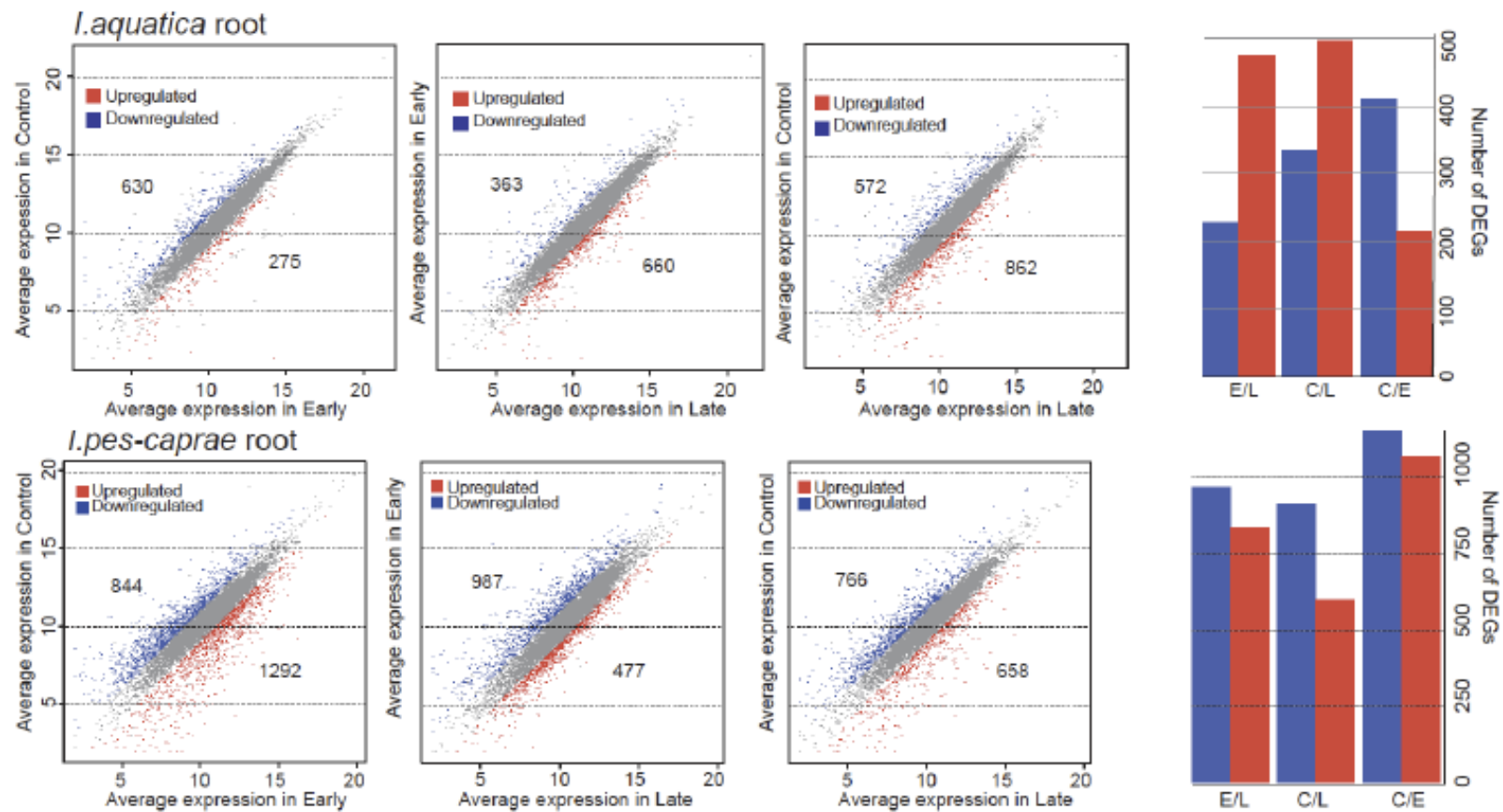


Figure 14: Differential gene expression analysis of Root samples from *I. aquatica* and *I. pes-caprae*. The figures show the numbers of differentially expressed genes in the Root in Early and Late samples compared to the Control samples, as well as Late sample compared to Early sample. The scatter plots on the left represent all genes, and the bar graphs on the right represent the number of genes up- and downregulated in each sample.

The functional annotation of genes in all samples was performed to determine the pfam accession and KO identifier associated with each gene based on their nucleotide sequence. These accessions were then used to study the pathways enriched in samples during salt-stress. The dcGO Enrichment online tool was used to identify the enrichment of pathways related to cellular components, biological processes, and molecular functions. Then, RStudio was used to visualize the up- and downregulated pathways (Figures 15-18). Pathways that are related to salinity-stress were identified and studied further to determine the fold changes of these pathways in all samples (Figures 19-20).

Analysis of leaf samples of *I. aquatica* and *I. pes-caprae* revealed several interesting pathways. *I. aquatica* leaves showed downregulation of photosynthesis related pathways (Figures 15 & 19). It also showed upregulation of abiotic-stress related pathways, while downregulation of other (Figures 15 & 19 ). However, *I. pes-caprae* leaves demonstrated upregulation of salt-stress related pathways as well as water deprivation pathways (Figures 17 & 19). The latter was upregulated by 2-4 folds in the Early samples (Figure 19). Since, salt stress leads to an increase of reactive oxygen species in cells, it is expected to detect upregulation of oxidoreduction related pathways. However, *I. aquatica* leaves showed little difference in the expression of oxidoreduction related pathways (Figures 15 & 19). On the other hand, *I. pes-caprae* demonstrated upregulation of pathways related to oxidoreduction, response to reactive oxygen species, and oxidoreduction coenzyme metabolic pathways (Figures 17 & 19). To maintain cellular homeostasis during salinity stress, plants utilize ion transport pathways, which is evident in *I. pes-caprae* leaves. *I. pes-caprae* displayed high expressed of pathways related to ion transport in all samples even Control (Figure 19).

However, *I. aquatica* leaves show downregulation of ion/anion transport pathways in the Early samples, followed by upregulation in Late samples only (Figure 19).

Analysis of root samples of *I. aquatica* and *I. pes-caprae* revealed some interesting pathways. In *I. aquatica* roots, there was some upregulation of pathways related to water deprivation and osmotic stress in the Early samples followed by downregulation of these pathways in the Late samples (Figures 16 & 20). *I. pes-caprae* root showed higher upregulation of pathways related to salt and osmotic stress, especially in the Early samples (2-4 folds upregulation) (Figure 20). Pathways related to reactive oxygen species were found to be upregulated in both plants; however, the fold changes were higher in *I. pes-caprae* root sample (Figures 17, 18, & 20). *I. aquatica* roots were found to upregulate several pathways related to transcription and RNA processing in the Late samples. This could be an indication that *I. aquatica* roots have a latent response to salinity compared to *I. pes-caprae*. Another interesting finding was the changes in expression of lipid-related pathways in both plants. During salt-stress, the increase of reactive oxygen species leads to the oxidation of some membrane lipids, which in turn damages the membrane fluidity and cell structure (Natera et al., 2016; Yu et al., 2020). Pathways related to lipid metabolism were upregulated in *I. pes-caprae* roots (all sample) but downregulated in *I. aquatica* roots Early sample (Figures 17, 18, & 20). Further analysis into the specific lipids and pathways that are differentially expressed between *I. aquatica* and *I. pes-caprae* can further clarify the differences in salt-tolerance of these plants. The analysis of pathways sheds light on many aspects of salt-tolerance that can be examined in more detail in future research.

## *I. aquatica* Leaf

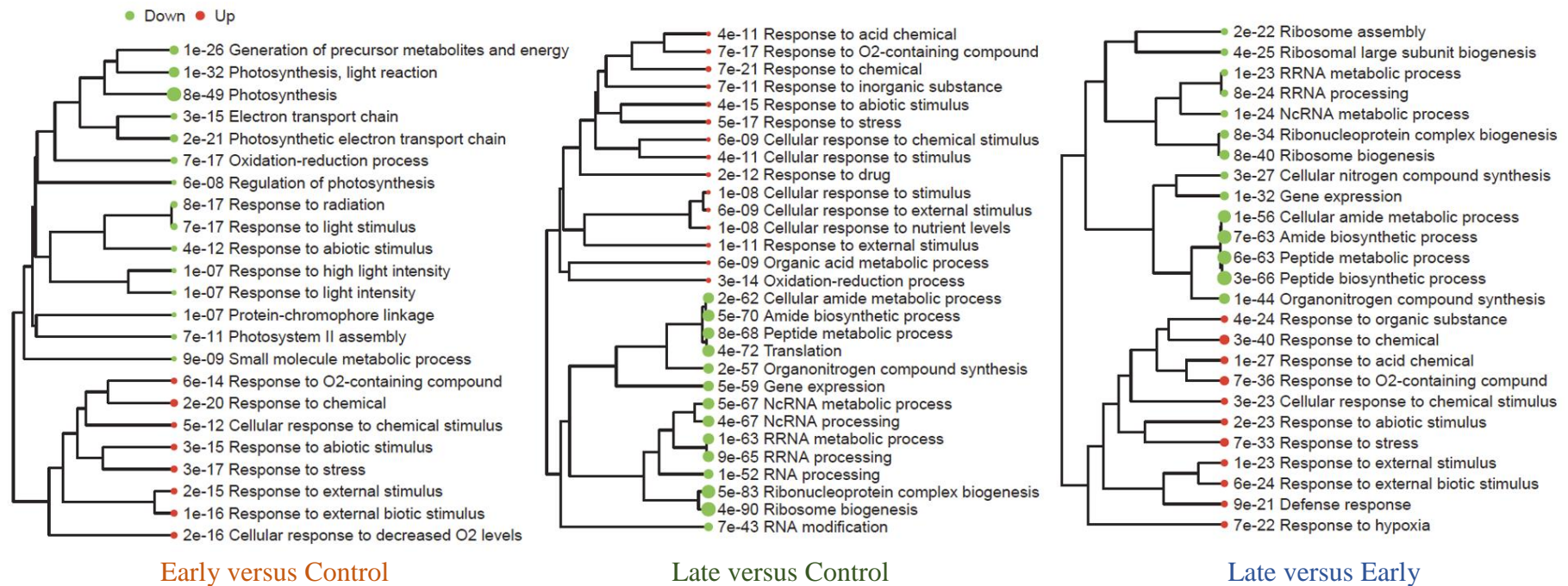


Figure 15: Differential expression of pathways in *I. aquatica* leaves. Both KO (from KEGG) and pfam (from Uniprot/EMBL-EBI) were determined for each gene then dcGO tool was used to determine all enriched pathways. The diagram shows the up- and downregulated pathways in all samples.

## *I. aquatica* Root

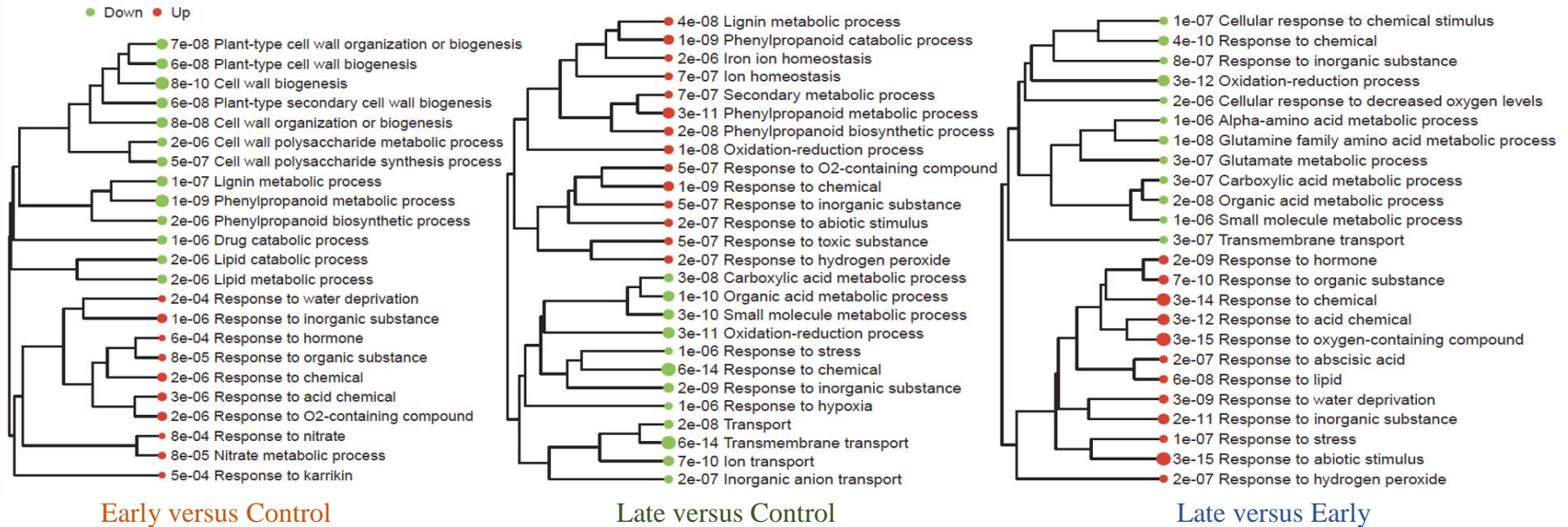


Figure 16: Differential expression of pathways in *I. aquatica* roots. Both KO (from KEGG) and pfam (from Uniprot/EMBL-EBI) were determined for each gene then dcGO tool was used to determine all enriched pathways. The diagram shows the up- and downregulated pathways in all samples.

## *I. pes-caprae* Leaf

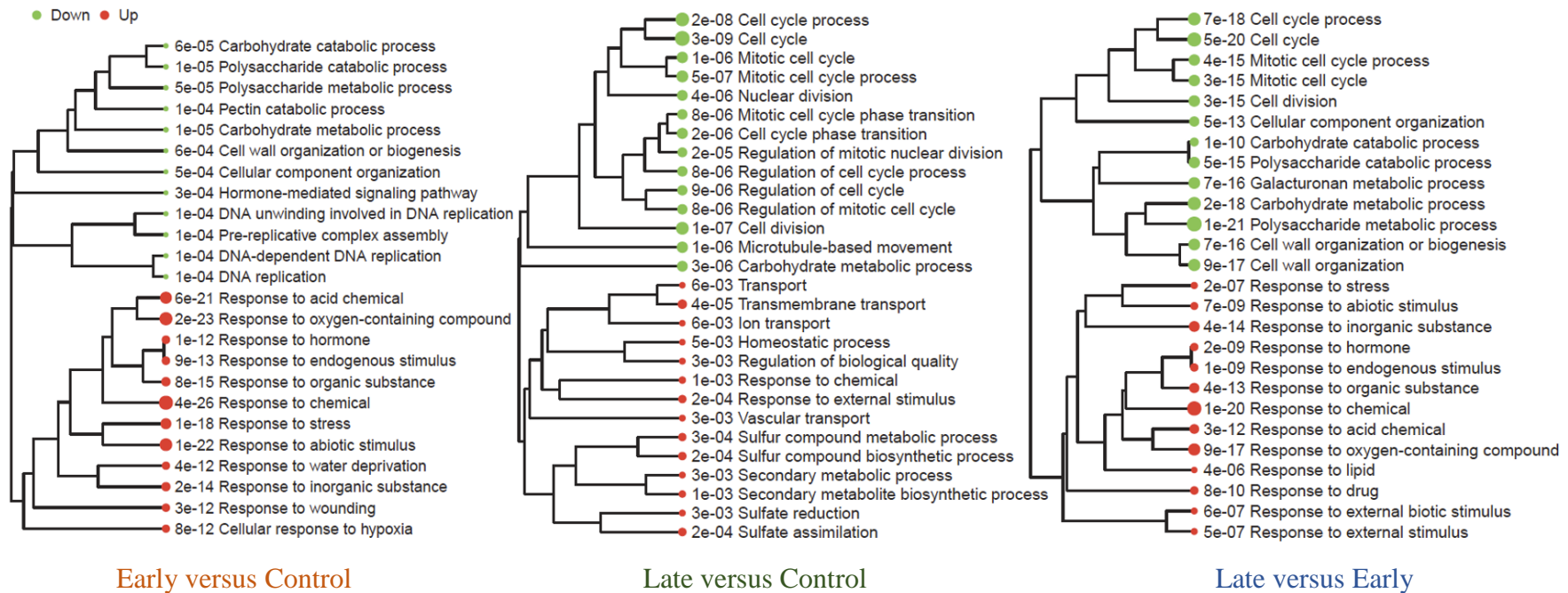


Figure 17: Differential expression of pathways in *I. pes-caprae* leaves. Both KO (from KEGG) and pfam (from Uniprot/EMBL-EBI) were determined for each gene then dcGO tool was used to determine all enriched pathways. The diagram shows the up- and downregulated pathways in all samples.

## *I. pes-caprae* Root

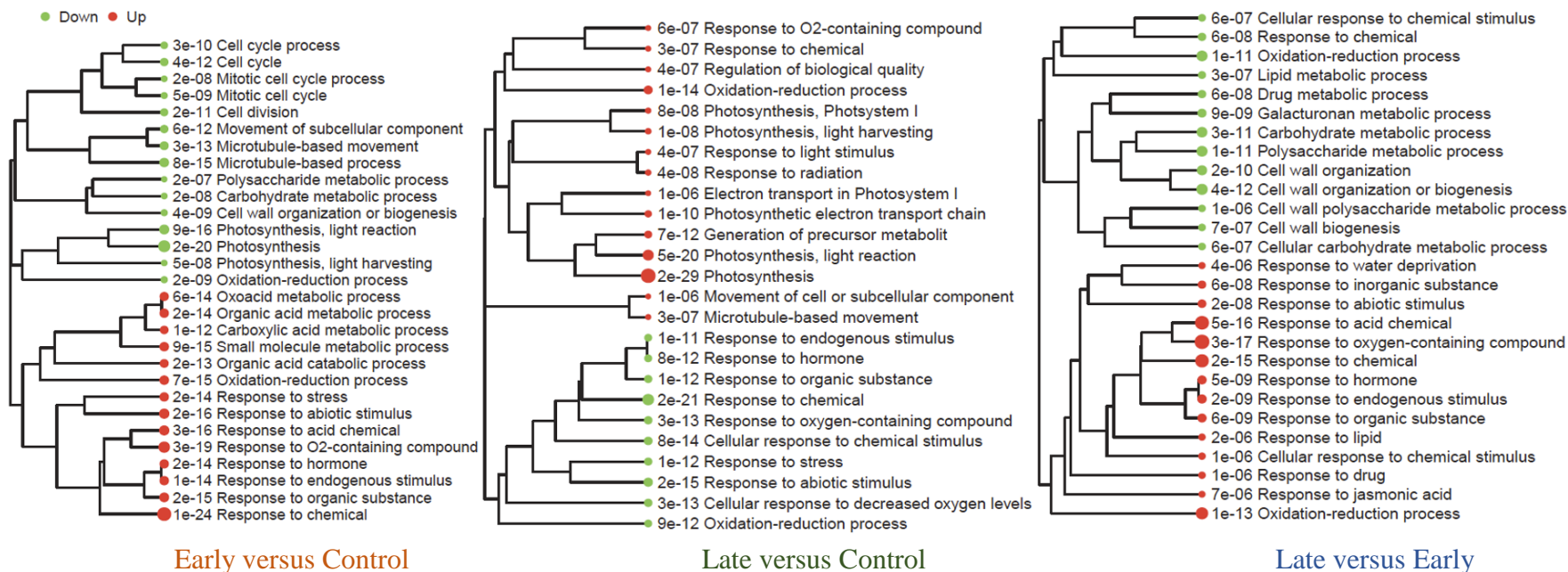
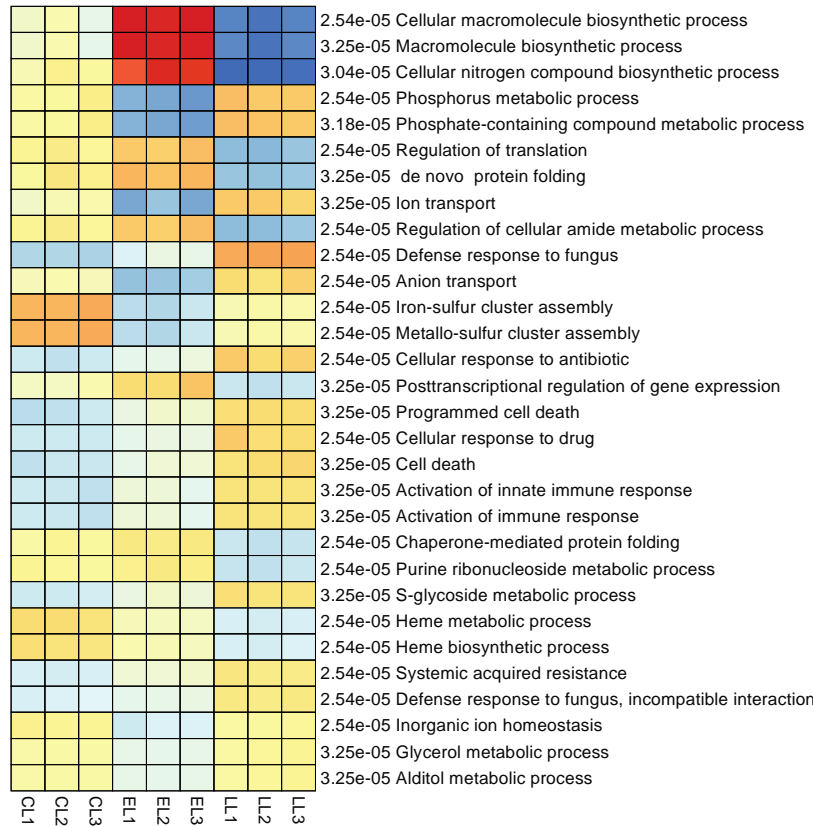


Figure 18: Differential expression of pathways in *I. pes-caprae* roots. Both KO (from KEGG) and pfam (from Uniprot/EMBL-EBI) were determined for each gene then dcGO tool was used to determine all enriched pathways. The diagram shows the up- and downregulated pathways in all samples.

### *I. aquatica* leaf



### *I. pes-caprae* leaf

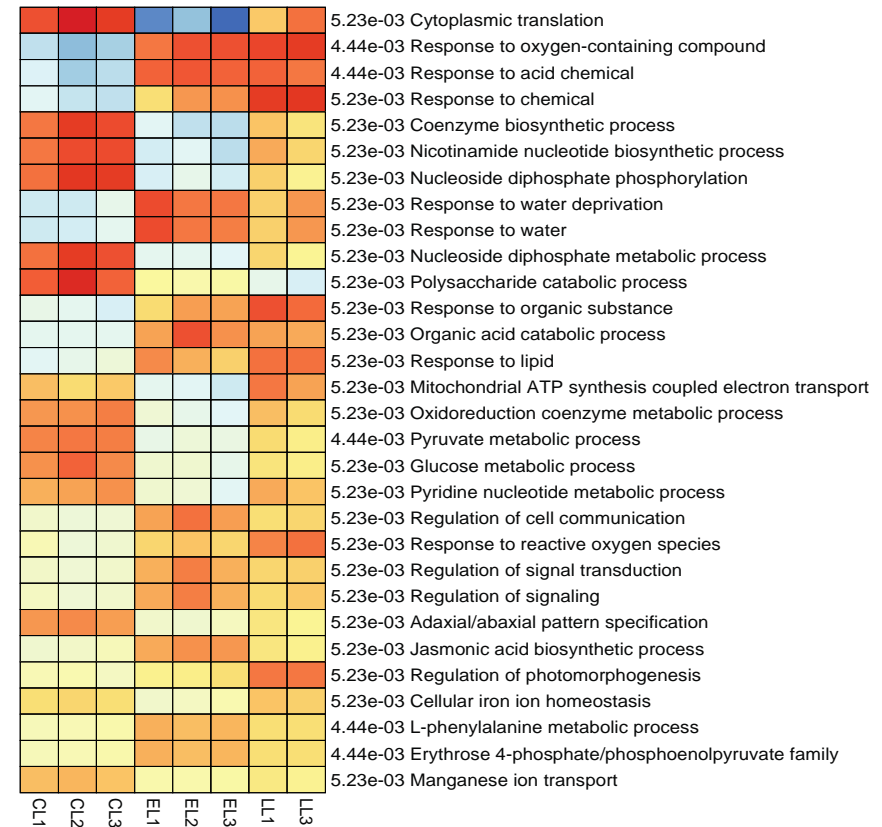
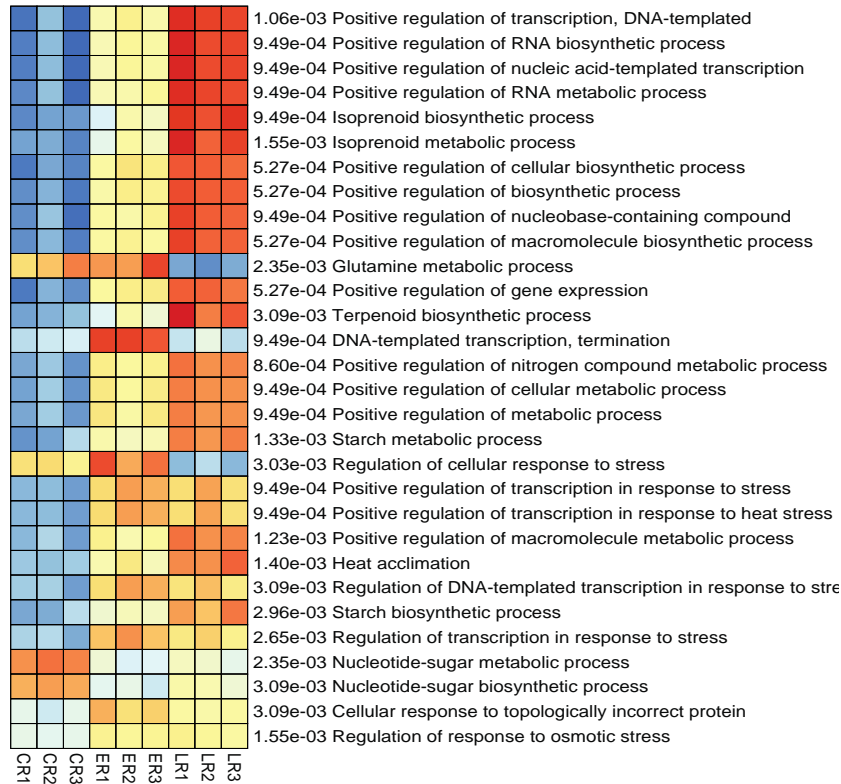


Figure 19: Differential gene expression of salt related identified pathways in Leaf samples. The heatmap represents the salt-related differentially expressed pathways in all samples (Control, Early and Late) in Leaf tissues.

*I.aquatica* root



*I.pes-caprae* root

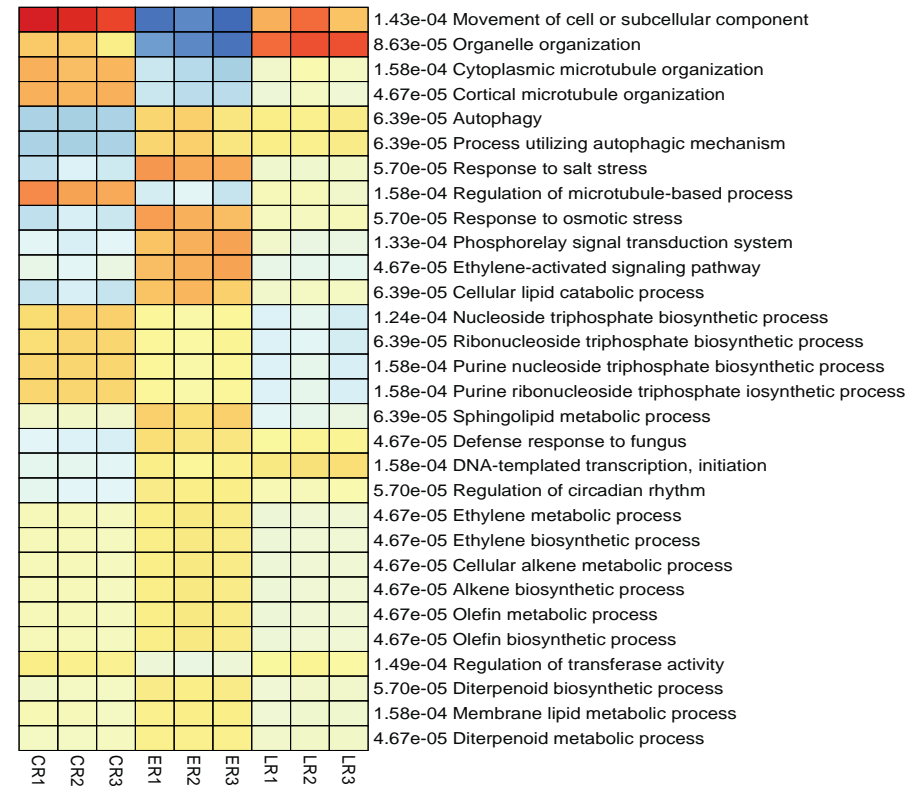


Figure 20: Differential gene expression of salt related identified pathways in Root samples. The heatmap represents the salt-related differentially expressed pathways in all samples (Control, Early and Late) in Root tissues.

Differentially expressed salt-related pathways were further analyzed, and genes belonging to these pathways were identified in all samples to study their individual expression profiles and determine candidate genes. The Venn diagram (Figure 21) shows the numbers of differential expressed salt-related genes in both plants as well as genes that were common and specific to each plant. As the figure shows, 79% of genes were common between the two plants in both tissues. However, there are genes that were found to be specific to *I. pes-caprae* roots (5.8%) and *I. aquatica* leaves (3.7%). These genes were analyzed to find the underlying genetic causes that might explain the difference in salt-tolerance of *I. aquatica* and *I. pes-caprae*. Some of these genes were chosen for qRT-PCR validation.

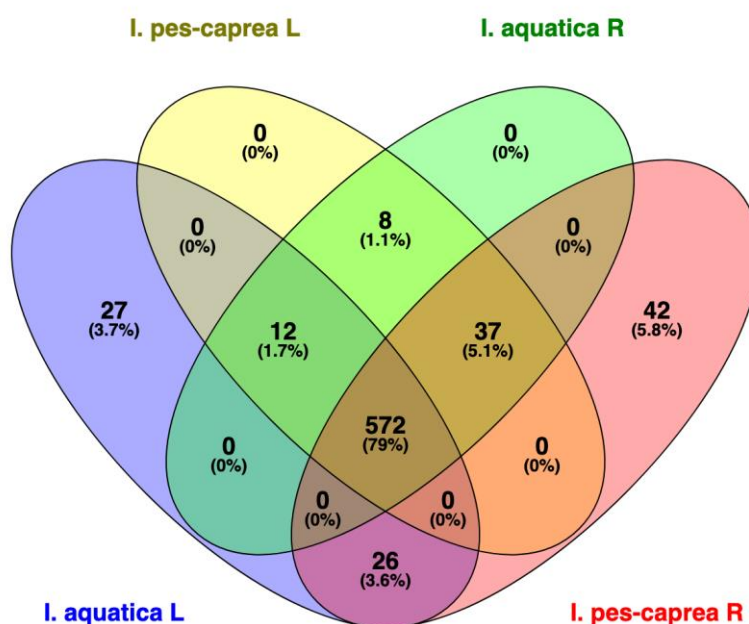


Figure 21: Venn Diagram showing all salt-related genes. *I. aquatica* Leaf (637), Root (627). *I. pes-caprae* Leaf (629), Root (677).

### 3.4.2 Analysis of miRNA

The number of miRNAs identified in both plants (Known and Novel miRNAs) are indicated in Appendix Figures 2 and 3. Differential expression analysis of known miRNAs through DESeq2 is shown in Figure 22. Several differentially expressed miRNAs that were detected have previously been studied in relation to stress. For example, miR165 and miR162 have been linked to response to stress in Rice (Bakhshi et al., 2016). The targets of known miRNAs were predicted using sequence homology and used for downstream analysis using the programs mentioned in Methods Section 2.3.2. The expression levels of miRNAs were compared with the expression levels of their predicted targets to identify possible miRNA/mRNA interactions.

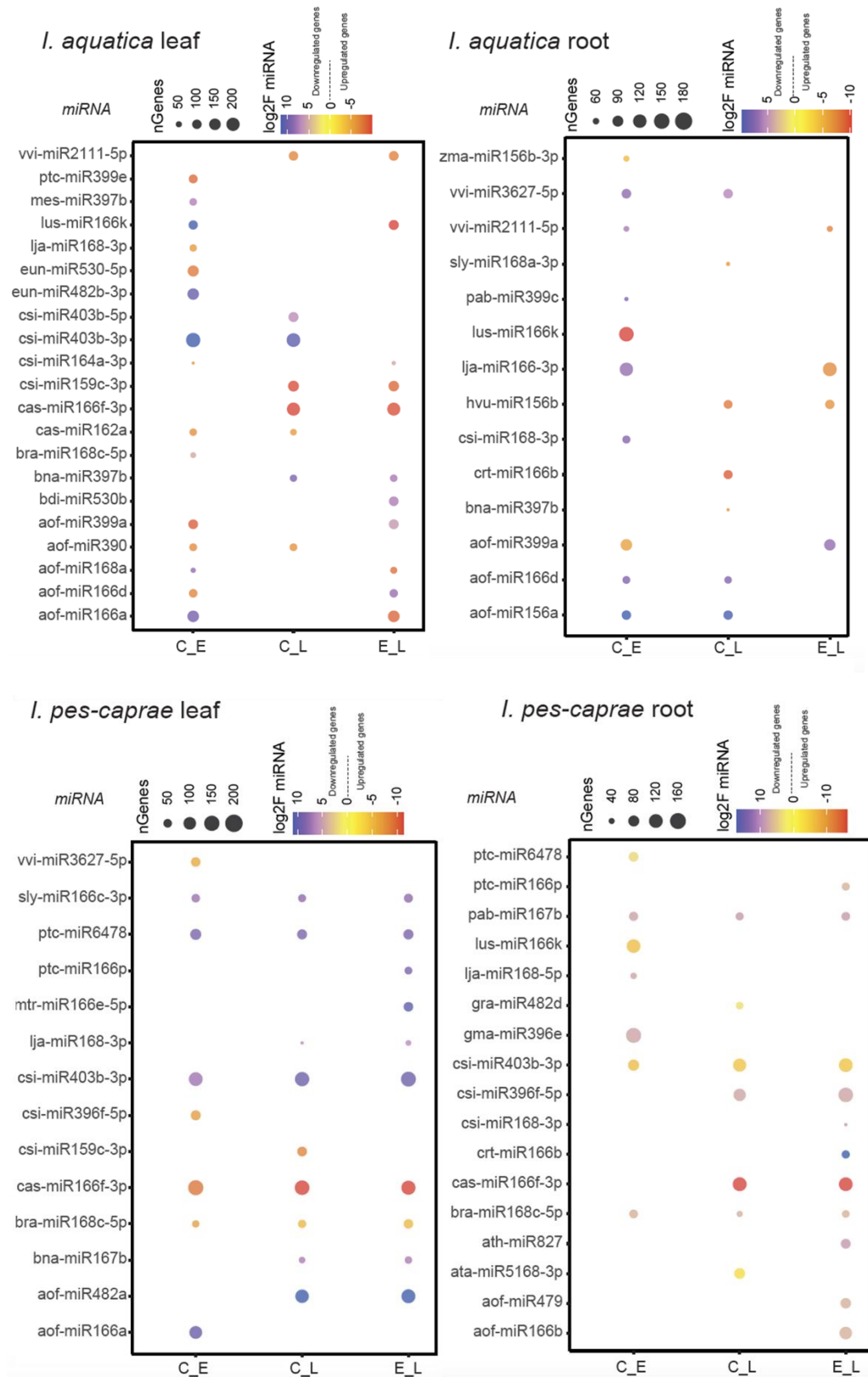


Figure 22: Differentially expressed miRNAs in all samples. The graph represents miRNA on the y-axis and the samples (Control versus Early, Control versus Late, and Early versus Late) on the x-axis. The size and color of the bubble indicates the level of differential expression.

### 3.4.3 Validation

To validate the results of the bioinformatics analysis, several differentially expressed genes were selected for quantitative Real-Time PCR (qRT-PCR) analysis (Figure 23; Appendix Table 4). These genes were selected because they showed an expression profile in *I. pes-caprae* that was different than *I. aquatica* under salinity. The fold changes were determined by comparing the expression of genes in the Early and Late samples to the Control sample (as described in Methods Section 2.3.3). The fold changes detected by qRT-PCR were compared to the fold changes determined using bioinformatics analysis of the transcriptomes. The regression analysis results indicate that bioinformatics analysis can be used to predict the actual fold changes of genes (Figure 24). To validate miRNA bioinformatics analysis, stem-loop primers were designed, and miRNA was extracted from the sample. However, the RT-qPCR is currently undergoing.

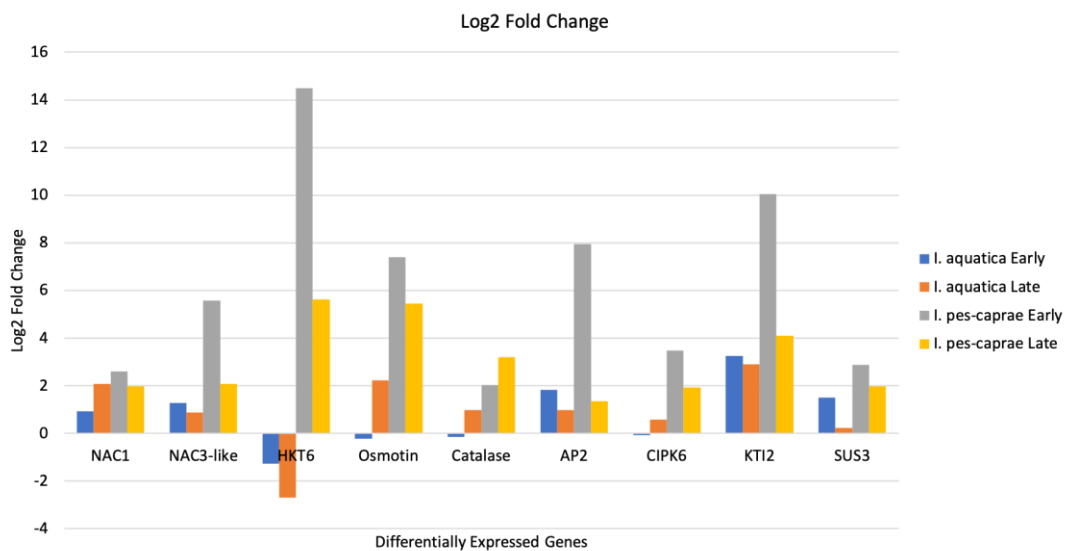


Figure 23: Log<sub>2</sub> fold changes detected with qRT-PCR.

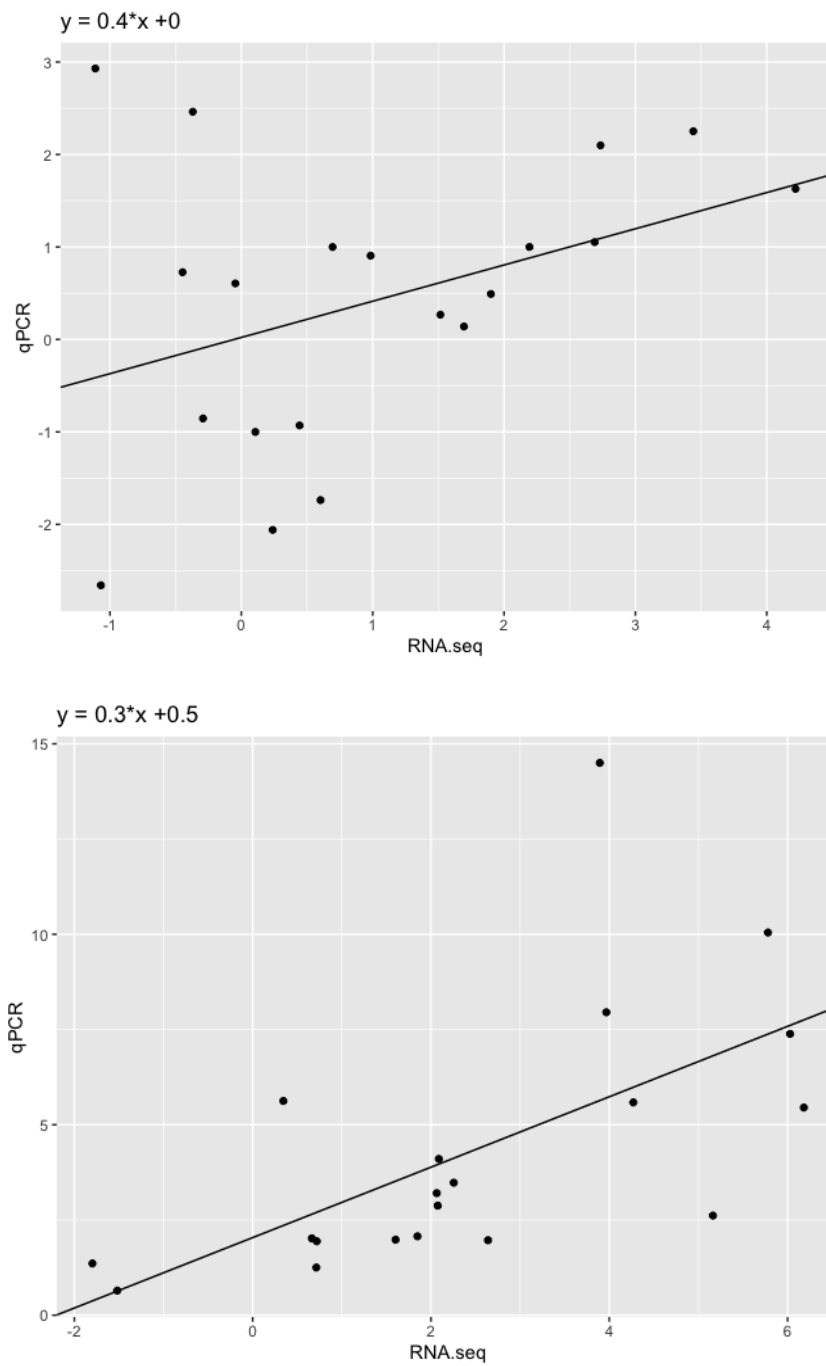


Figure 24: Regression analysis of *I. aquatica* (top) and *I. pes-caprae* (bottom)

## Chapter 4: Discussion

The result of the physiological analysis of *I. aquatica* and *I. pes-caprae* under stress show a crucial difference between the two plants. *I. pes-caprae* is able to regulate its cellular homeostasis during salinity stress by maintaining a stable ratio of ions in its cells (mainly  $\text{Na}^+/\text{Cl}^-$ ). It was also able to keep oxidative damage in its tissues to relatively low levels, which helped the plant maintain its photosynthesis rates. On the other hand, *I. aquatica* was not able to maintain cellular homeostasis to the same degree and thus experienced much more severe effects during salinity stress. The analysis of the transcriptome and miRNA profiles of both plants corroborate the results of the physiological measurements. *I. pes-caprae* enriches pathways relating to oxidative damage and ion homeostasis in a higher level than *I. aquatica*. *I. pes-caprae* also showed enrichment in the expression of some genes that might be related to its response to salinity stress. Thousands of genes were determined to be differentially expressed during salinity in the two plants. Many miRNA-mRNA interactions were predicted in the plants as well. These results represent a great resource in finding the underlying genetic mechanisms of salt tolerance. Further analysis of these genes and miRNAs that regulate the plants' adaptation to salinity will lead to the identification of genetic components that can be used to enhance *I. aquatica*'s salt tolerance levels. This section will focus on two prominent genes (HKT and NAC) as they have shown to be differentially expressed during salinity stress, and their expression profiles differ between *I. aquatica* and *I. pes-caprae*.

#### 4.1 HKT Gene

The transcriptome and miRNA analysis of both plants revealed some genes that might be the cause of the disparity in salt tolerance between the two plants. One of these gene encodes High-Affinity Potassium Transporter (HKT). Potassium transporters play an important role in maintaining cellular homeostasis during salt stress. In *I. pes-caprae*, differential gene expression analysis revealed significant upregulation of an HKT gene (4 folds in the Early stage). This gene was also found in *I. aquatica*; however, it was not expressed in the Early stage and downregulated (-1.3 fold) in the Late stage. Both genes were matched to HKT1 in *A. thaliana* and a putative HKT6 in other Ipomoea species (Figure 25). Validation with qRT-PCR revealed that *I. pes-caprae* HKT was actually 14 folds upregulated in the Early stage (compared to 4 predicted), and 5.6 fold upregulated in the Late stage (no fold change predicted).

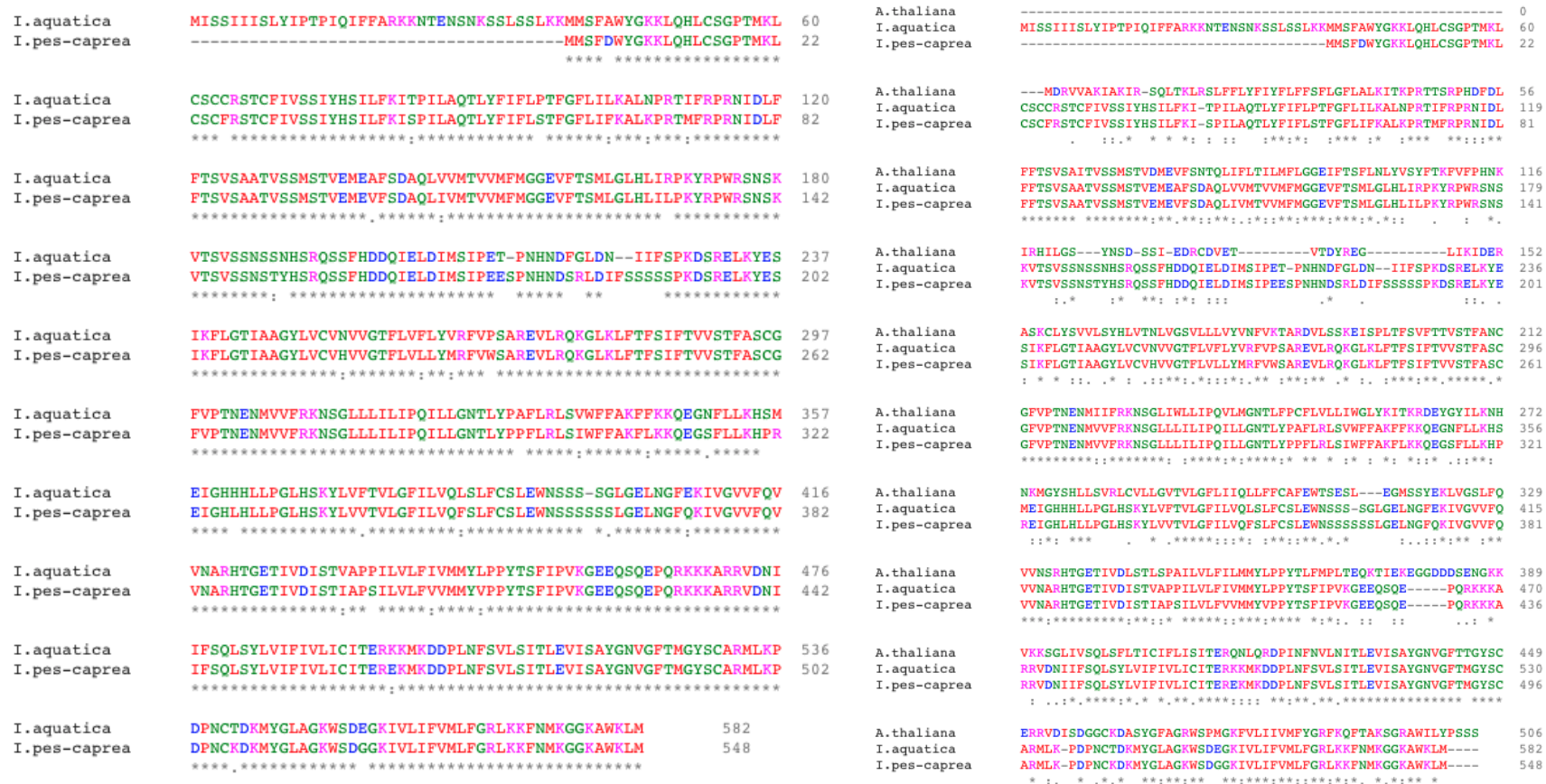


Figure 25: Alignment of HKT protein sequence. The figure shows the alignment HKT amino acid sequences from *I. aquatica* and *I. pes-caprae* (left) and *Arabidopsis thaliana* (right). The figure was generated using Clustal omega alignment tool.

Analysis of miRNAs revealed that in *I. aquatica*, HKT gene is predicted to be targeted by the miRNA genes miR159e; however, the detected copy number of these miRNAs was too low to undergo statistical analysis (Figure 26). HKT in *I. aquatica* may also be targeted miR166a and miR165a to a lesser degree based to sequence similarity between these miRNAs and HKT gene. On the other hand, *I. pes-caprae* HKT gene is predicted to be targeted by miR396a, which is not significantly expressed in the Early stage but is downregulated (-5.5 fold) in the Late stage. Validation of these fold changes of miRNAs with stem-loop qRT-PCR is currently undergoing; and further research is needed to confirm this predicted miRNA-mRNA interaction.

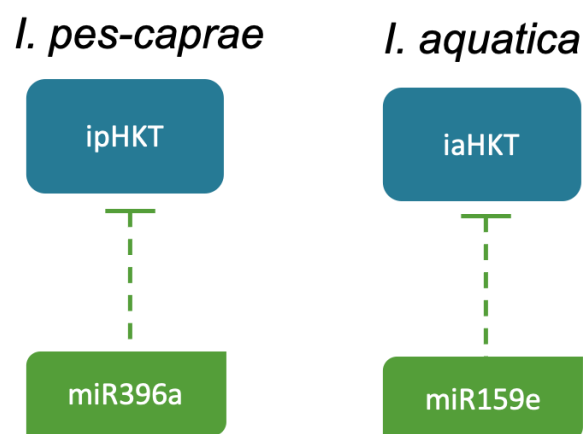


Figure 26: Predicted interaction of miRNAs with HKT gene in *I. aquatica* and *I. pes-caprae*. This miRNA-mRNA association was predicted by analyzing nucleotide sequences of the genes and miRNAs.

The upregulation of HKT gene in *I. pes-caprae* may be linked to the downregulation of miR396a. The miRNA-mRNA interaction for HKT in *I. aquatica* is not fully understood yet; however, overexpression of HKT in *I. aquatica* could potentially lead to enhanced salt-tolerance.

## 4.2 NAC3-like Gene

Another gene identified through transcriptome analysis is NAC3-like transcription factor found in both *I. aquatica* and *I. pes-caprae*. The differential expression analysis of the transcriptome revealed a NAC-domain-containing gene that is upregulated in response to salinity in *I. pes-caprae* by 4.3 folds in the Early stage and 1.8 folds in the Late stage. In *I. aquatica*, this gene was upregulated by 1.9 folds in the Early stage and unchanged in the Late stage. The sequence of this genes corresponds to NAC3 gene in *Arabidopsis thaliana* (AT3G15500), also known as NAC055, with 70.56% identity (Figure 27).

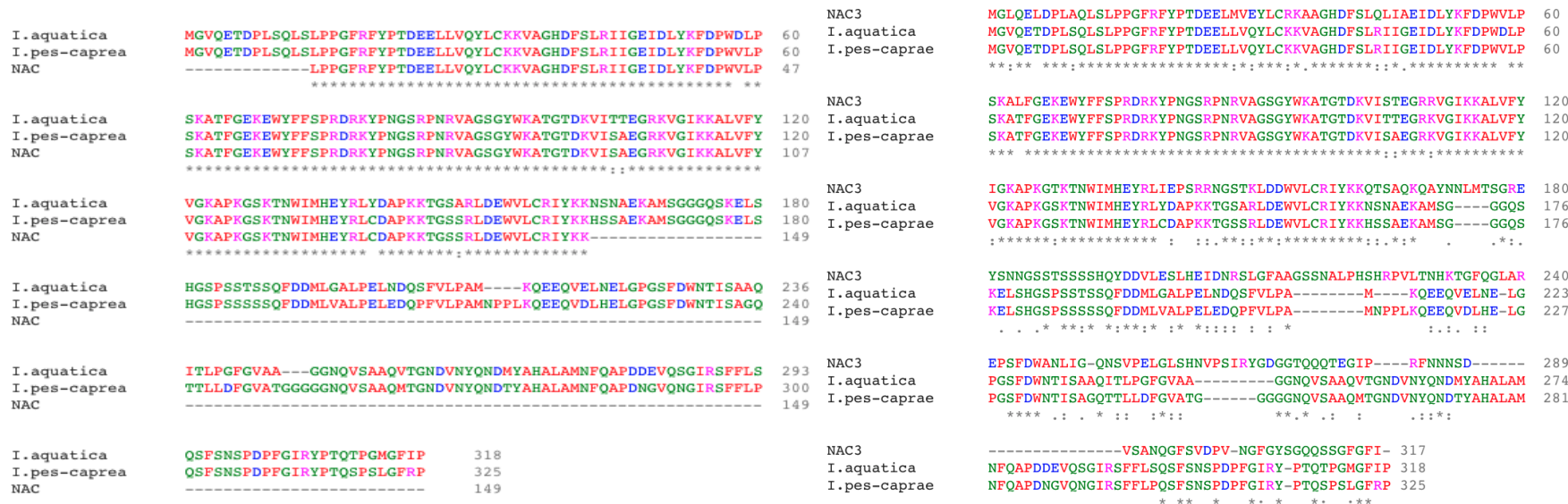


Figure 27: Alignment of protein sequence of NAC3-like. The figure shows the alignment NAC3-like amino acid sequences from *I. aquatica* and *I. pes-caprae* with the conserved NAC domain (left), and with *Arabidopsis thaliana* NAC3 (right). Alignments were generated using Clustal omega tool.

Validation of the NAC3-like gene expression through qRT-PCR revealed that the predicted fold changes were slightly lower, but not significantly different, than the detected fold changes. According to the qRT-PCR results, NAC3-like gene was upregulated by 5.6 folds in the Early (compared to 4.3 predicted) stage and 2 folds in the Late (compared to 1.8 predicted).

Through miRNA target analysis, it was determined that this NAC3-like gene in *I. pes-caprae* may be targeted by some miRNA genes including miR167, which is similar to miR162 in sequence. Analysis of miR167 was not conclusive due to low copy number of the sequence (Figure 28). However, miR162 was revealed to be downregulated in *I. pes-caprae* (-7.7 fold in Early stage; -6.3 fold in Late stage). The potential interaction between *I. pes-caprae* NAC3-like and miR162 is not confirmed yet and the miRNA validation using qRT-PCR is undergoing. However, this finding presents an interesting possible miRNA-mRNA interaction in *I. pes-caprae*. Due to the complexity and low expression of miRNA, the validation of these results is difficult yet undergoing.

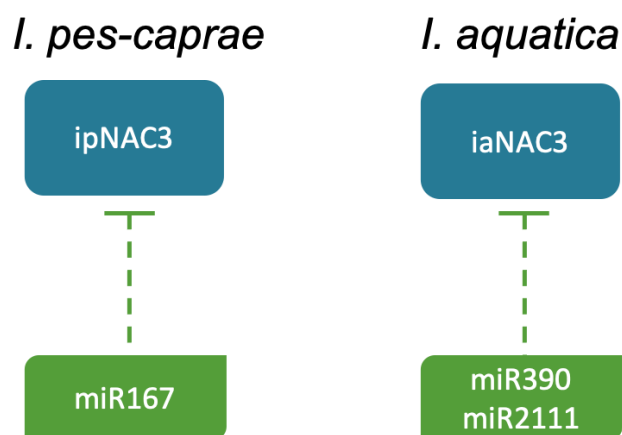


Figure 28: Predicted interaction of miRNAs with NAC3-like gene in *I. aquatica* and *I. pes-caprae*. This miRNA-mRNA association was predicted by analyzing nucleotide sequences of the genes and miRNAs

The miRNA target analysis of *I. aquatica* gene sequences revealed that NAC3-like was not targeted by miR167, but it was targeted by two different miRNA genes (miR2111d and miR390) (Figure 23). Differential expression analysis of both miRNAs revealed that neither was significantly expressed in any stage of the experiment. This could be due to the low copy number detection, which resulted in inconclusive statistical analysis; or it could be because the miRNAs are not responsive to salt-stress. Further analysis is needed to discern the interactions between these miRNAs and the *I. aquatica* NAC3-like gene. Regardless, this NAC3-like gene is linked to the salinity response in *I. pes-caprae* and could be used to enhance *I. aquatica*'s tolerance to salinity through overexpression.

#### **4.3 Photosynthesis Pathways**

Photosynthesis is one of the key pathways affected by salinity. The effects can either be caused by inducing stomatal closure, which in turn reduces intercellular CO<sub>2</sub>, or it can be caused by inhibition of chlorophyll production (Liu et al., 2011). Differences in these factors (Table 1) can explain *I. pes-caprae*'s ability to grow under salinity conditions. The results indicate that *I. pes-caprae* is able to recover its photosynthesis rate under salinity conditions, as opposed to *I. aquatica*. Moreover, *I. pes-caprae* is able to reduce its water-loss by decreasing stomatal conductance as well as maintaining its chlorophyll content. These phenotypic responses are confirmed by transcriptome analysis, which shows that photosynthesis genes are downregulated in *I. aquatica* throughout the experiment, as opposed to *I. pes-caprae*. The transcriptome analysis also reveals upregulation of photosynthesis related pathways in *I. pes-caprae* roots, but not in *I. aquatica*. Previous studies indicate that photosynthesis in non-leaf tissue can enhance the plant's ability to survive during abiotic stress conditions (Henry

et al., 2020). This might be a key factor in salt-tolerance in *I. pes-caprae* compared to *I. aquatica*. Stress induces photosynthesis in roots through C<sub>4</sub> pathway rather than C<sub>3</sub> (Henry et al., 2020). Further analysis into the photosynthesis pathways of *I. aquatica* and *I. pes-caprae* is needed to elucidate the differences in these pathways in both leaves and roots.

Table 1: Summary of the physiological response to salinity in relation to photosynthesis

<b>Physiology</b>	<i>Ipomoea aquatica</i>	<i>Ipomoea pes-caprae</i>
<b>Photosynthesis Rate</b>	Reduced throughout the experiment	Reduced in the early stage then increased slightly
<b>Stomatal Conductance</b>	Increased in the early stages then decreased	Decreased throughout the experiment
<b>Intercellular CO<sub>2</sub></b>	Increased in the late stage only	Increased in the Early stage then reduced in the late stage
<b>Chlorophyll content</b>	Reduced throughout the experiment	Unchanged

## Chapter 5: Conclusion

The results of this study highlight many important differences in the salinity stress response of *I. aquatica* and *I. pes-caprae*. The physiological analysis revealed that maintaining low levels of reactive oxygen species and stable ion concentrations helped *I. pes-caprae* maintain its photosynthetic rates. The stark difference in the two plants' cellular homeostasis indicate a fundamental difference than can be explored in the effort to enhance *I. aquatica*'s salt tolerance. The analysis of the differentially expressed mRNAs and miRNAs revealed the underlying genetic differences between the two plants' response to salinity. Though the genetic differences are far too many to be explored in the scope of this study, several genes were identified as promising candidate genes for *I. aquatica* transformation.

### 5.1 Research Implications

This research generated a large amount of data including the full salt-related expression of mRNA and miRNA in *I. aquatica* and *I. pes-caprae* leaf and root tissue. This resulted in the identification of thousands of differentially expressed genes and miRNAs in both plants. The plethora of information generated by this study can be utilized in future research into salt-related genes and miRNAs. The lncRNAs of both plants are being analyzed as well, which will only increase the knowledge of genetic mechanisms of salt-tolerance in plants. Analyzing the vast network of interactions between mRNAs and Nc-RNAs is crucial as it will allow for a more fine-tuned approach in *I. aquatica* genetic engineering. Comparative genomic analysis of both plants can also lead to identification of differences in regulatory regions

(like promoters) or gene structures than can further enhance the knowledge of salt-tolerance mechanisms.

The results of this study will undoubtedly lead to the identification of more genes than can be used in genetic engineering studies to enhance the salt-tolerance of crops. The genes discussed in this study (HKT and NAC) can be used to genetically engineer *I. aquatica* to increase its salt tolerance levels. These genes can be used to improve *I. aquatica*, as well as other Ipomoea species of great value like sweet potato, which also has great economic value. Further studies into other Ipomoea species that build on the information generated from this research project are therefore necessary.

## References

- Abdelfattah, M. A., & Shahid, S. A. (2014). Spatial Distribution of Soil Salinity and Management Aspects in the Northern United Arab Emirates. In M. A. Khan, B. Böer, M. Öztürk, T. Z. Al Abdessalaam, M. Clüsener-Godt, & B. Gul (Eds.), *Sabkha Ecosystems: Volume IV: Cash Crop Halophyte and Biodiversity Conservation* (pp. 1–22). Springer Netherlands. [https://doi.org/10.1007/978-94-007-7411-7\\_1](https://doi.org/10.1007/978-94-007-7411-7_1)
- Agathokleous, E., Feng, Z., & Peñuelas, J. (2020). Chlorophyll hormesis: Are chlorophylls major components of stress biology in higher plants? *The Science of the Total Environment*, 726(138637), 1–9. <https://doi.org/10.1016/j.scitotenv.2020.138637>
- Al Yamani, W., & Athamneh, B. (2017). *Abu Dhabi State of Environment Report 2017*. Environment Agency – Abu Dhabi. Retrieved October 1, 2018, from [https://www.soe.ae/wp-content/uploads/2017/11/Soil\\_English.pdf](https://www.soe.ae/wp-content/uploads/2017/11/Soil_English.pdf)
- Altschul, S. F., Gish, W., Miller, W., Myers, E. W., & Lipman, D. J. (1990). Basic local alignment search tool. *Journal of Molecular Biology*, 215(3), 403–410. [https://doi.org/10.1016/S0022-2836\(05\)80360-2](https://doi.org/10.1016/S0022-2836(05)80360-2)
- Arnnok, P., Ruangviriyachai, C., Mahachai, R., Techawongstien, S., & Chanthai, S. (2010). Optimization and determination of polyphenol oxidase and peroxidase activities in hot pepper (*Capsicum annum* L.) pericarb. *International Food Research Journal*, 17(2), 385–392.
- Austin, D. F. (2007). Water Spinach (*Ipomoea aquatica*, Convolvulaceae): A food gone wild. *Ethnobotany Research and Applications*, 5(0), 123–146.
- Bai, K. V., Magoon, M. L., & Krishnan, R. (1969). Cytological And Morphological Studies Of Diploid And Tetraploid Species Of *Ipomoea Biloba*. *The Japanese Journal of Genetics*, 44(5), 329–338. <https://doi.org/10.1266/jjg.44.329>
- Bakhshi, B., Mohseni Fard, E., Nikpay, N., Ebrahimi, M. A., Bihamta, M. R., Mardi, M., & Salekdeh, G. H. (2016). MicroRNA Signatures of Drought Signaling in Rice Root. *PLoS ONE*, 11(6), 1–25. <https://doi.org/10.1371/journal.pone.0156814>
- Baldoni, E., Bagnaresi, P., Locatelli, F., Mattana, M., & Genga, A. (2016). Comparative Leaf and Root Transcriptomic Analysis of two Rice Japonica Cultivars Reveals Major Differences in the Root Early Response to Osmotic Stress. *Rice*, 9(1), 1–20. <https://doi.org/10.1186/s12284-016-0098-1>

- Betel, D., Koppal, A., Agius, P., Sander, C., & Leslie, C. (2010). Comprehensive modeling of microRNA targets predicts functional non-conserved and non-canonical sites. *Genome Biology*, *11*(8), 1–14. <https://doi.org/10.1186/gb-2010-11-8-r90>
- Bolger, A. M., Lohse, M., & Usadel, B. (2014). Trimmomatic: A flexible trimmer for Illumina sequence data. *Bioinformatics*, *30*(15), 2114–2120. <https://doi.org/10.1093/bioinformatics/btu170>
- Buchfink, B., Xie, C., & Huson, D. H. (2015). Fast and sensitive protein alignment using DIAMOND. *Nature Methods*, *12*(1), 59–60. <https://doi.org/10.1038/nmeth.3176>
- Cakmak, I., & Marschner, H. (1992). Magnesium deficiency and high light intensity enhance activities of superoxide dismutase, ascorbate peroxidase, and glutathione reductase in bean leaves. *Plant Physiology*, *98*(4), 1222–1227. <https://doi.org/10.1104/pp.98.4.1222>
- Chen, C., Ridzon, D. A., Broomer, A. J., Zhou, Z., Lee, D. H., Nguyen, J. T., Barbisin, M., Xu, N. L., Mahuvakar, V. R., Andersen, M. R., Lao, K. Q., Livak, K. J., & Guegler, K. J. (2005). Real-time quantification of microRNAs by stem-loop RT-PCR. *Nucleic Acids Research*, *33*(20), 179–188. <https://doi.org/10.1093/nar/gni178>
- Dai, X., Zhuang, Z., & Zhao, P. X. (2018). psRNATarget: A plant small RNA target analysis server. *Nucleic Acids Research*, *46*(W1), 49–54. <https://doi.org/10.1093/nar/gky316>
- Deng, P., Wang, L., Cui, L., Feng, K., Liu, F., Du, X., Tong, W., Nie, X., Ji, W., & Weining, S. (2015). Global Identification of MicroRNAs and Their Targets in Barley under Salinity Stress. *PLOS ONE*, *10*(9), 1–20. <https://doi.org/10.1371/journal.pone.0137990>
- Dias, K. G. de L., Guimarães, P. T. G., Neto, A. E. F., Silveira, H. R. O. de, & Lacerda, J. J. de J. (2017). Effect of Magnesium on Gas Exchange and Photosynthetic Efficiency of Coffee Plants Grown under Different Light Levels. *Agriculture*, *7*(10), 1–11. <https://doi.org/10.3390/agriculture7100085>
- Environment Agency - Abu Dhabi. (2019). *Soil Salinity Management Plan* (pp. 1–136). Environment Agency. Retrieved December 1, 2020, from <https://www.ead.gov.ae/storage/soil%20Salinity%20low%20res%20English.pdf>

- Fang, H., & Gough, J. (2013). dcGO: Database of domain-centric ontologies on functions, phenotypes, diseases and more. *Nucleic Acids Research*, *41*(D1), 536–544. <https://doi.org/10.1093/nar/gks1080>
- Flowers, T., & Colmer, T. (2008). Salinity tolerance in halophytes. *New Phytologist*, *179*(4), 945–963. <https://doi.org/10.1111/j.1469-8137.2008.02531.x>
- Henry, R. J., Furtado, A., & Rangan, P. (2020). Pathways of Photosynthesis in Non-Leaf Tissues. *Biology*, *9*(12), 438–441. <https://doi.org/10.3390/biology9120438>
- Hossain, M. S., & Dietz, K.-J. (2016). Tuning of Redox Regulatory Mechanisms, Reactive Oxygen Species and Redox Homeostasis under Salinity Stress. *Frontiers in Plant Science*, *7*(548), 1–15. <https://doi.org/10.3389/fpls.2016.00548>
- Hu, Y., & Schmidhalter, U. (2004). Limitation of Salt Stress to Plant Growth. In *Plant Toxicology* (4th ed., pp. 191–224). Retrieved September 1, 2018, from [https://www.researchgate.net/publication/283678992\\_Limitation\\_of\\_Salt\\_Stress\\_to\\_Plant\\_Growth](https://www.researchgate.net/publication/283678992_Limitation_of_Salt_Stress_to_Plant_Growth)
- Huang, Y.-Y., Shen, C., Chen, J.-X., He, C.-T., Zhou, Q., Tan, X., Yuan, J.-G., & Yang, Z.-Y. (2016). Comparative Transcriptome Analysis of Two *Ipomoea aquatica* Forsk. Cultivars Targeted To Explore Possible Mechanism of Genotype-Dependent Accumulation of Cadmium. *Journal of Agricultural and Food Chemistry*, *64*(25), 5241–5250. <https://doi.org/10.1021/acs.jafc.6b01267>
- Imadi, S. R., Shah, S. W., Kazi, A. G., Azooz, M. M., & Ahmad, P. (2016). Chapter 18—Phytoremediation of Saline Soils for Sustainable Agricultural Productivity. In P. Ahmad (Ed.), *Plant Metal Interaction* (pp. 455–468). Elsevier. <https://doi.org/10.1016/B978-0-12-803158-2.00018-7>
- JHU. (2020). *StringTie2*. The Center for Computational Biology at Johns Hopkins University. Retrieved May 1, 2020, from <https://ccb.jhu.edu/software/stringtie/dl/prepDE.py>
- Kim, D., Paggi, J. M., Park, C., Bennett, C., & Salzberg, S. L. (2019). Graph-based genome alignment and genotyping with HISAT2 and HISAT-genotype. *Nature Biotechnology*, *37*(8), 907–915. <https://doi.org/10.1038/s41587-019-0201-4>

- Kovaka, S., Zimin, A. V., Pertea, G. M., Razaghi, R., Salzberg, S. L., & Pertea, M. (2019). Transcriptome assembly from long-read RNA-seq alignments with StringTie2. *Genome Biology*, 20(1), 278. <https://doi.org/10.1186/s13059-019-1910-1>
- Kozomara, A., Birgaoanu, M., & Griffiths-Jones, S. (2019). miRBase: From microRNA sequences to function. *Nucleic Acids Research*, 47(D1), D155–D162. <https://doi.org/10.1093/nar/gky1141>
- Li, H., Handsaker, B., Wysoker, A., Fennell, T., Ruan, J., Homer, N., Marth, G., Abecasis, G., Durbin, R., & 1000 Genome Project Data Processing Subgroup. (2009). The Sequence Alignment/Map format and SAMtools. *Bioinformatics*, 25(16), 2078–2079. <https://doi.org/10.1093/bioinformatics/btp352>
- LI-COR Biosciences. (2020). *Using the LI-6800 Portable Photosynthesis System*. LI-COR Biosciences. Retrieved June 1, 2020, from <https://licor.app.boxenterprise.net/s/rjj78fc7anvaxyfu64zzfdyd9ydc4gvk>
- Liu, Yang, Dai, X., Zhao, L., Huo, K., Jin, P., Zhao, D., Zhou, Z., Tang, J., Xiao, S., & Cao, Q. (2020). RNA-seq reveals the salt tolerance of *Ipomoea pes-caprae*, a wild relative of sweet potato. *Journal of Plant Physiology*, 255(153276), 1–10. <https://doi.org/10.1016/j.jplph.2020.153276>
- Liu, Yiming, Du, H., Wang, K., Huang, B., & Wang, Z. (2011). Differential Photosynthetic Responses to Salinity Stress between Two Perennial Grass Species Contrasting in Salinity Tolerance. *HortScience*, 46(2), 311–316. <https://doi.org/10.21273/HORTSCI.46.2.311>
- Love, M., Anders, S., & Huber, W. (2020). *Analyzing RNA-seq data with DESeq2*. Retrieved May 1, 2020, from <http://www.bioconductor.org/packages/release/bioc/vignettes/DESeq2/inst/doc/DESeq2.html>
- Love, M., Huber, W., & Anders, S. (2014). Moderated estimation of fold change and dispersion for RNA-seq data with DESeq2. *Genome Biology*, 15(550), 1–21. <https://doi.org/10.1186/s13059-014-0550-8>
- Meira, M., Silva, E. P. da, David, J. M., & David, J. P. (2012). Review of the genus *Ipomoea*: Traditional uses, chemistry and biological activities. *Revista Brasileira de Farmacognosia*, 22(3), 682–713. <https://doi.org/10.1590/S0102-695X2012005000025>
- Mishra, A., & Tanna, B. (2017). Halophytes: Potential Resources for Salt Stress Tolerance Genes and Promoters. *Frontiers in Plant Science*, 8(829), 1–10. <https://doi.org/10.3389/fpls.2017.00829>

- Monnet-Tschudi, F., Zurich, M.-G., Boschat, C., Corbaz, A., & Honegger, P. (2006). Involvement of Environmental Mercury and Lead in the Etiology of Neurodegenerative Diseases. *Reviews on Environmental Health*, 21(2), 105. <https://doi.org/10.1515/REVEH.2006.21.2.105>
- Moriya, Y., Itoh, M., Okuda, S., Yoshizawa, A. C., & Kanehisa, M. (2007). KAAS: An automatic genome annotation and pathway reconstruction server. *Nucleic Acids Research*, 35(2), W182-185. <https://doi.org/10.1093/nar/gkm321>
- Natera, S. H. A., Hill, C. B., Rupasinghe, T. W. T., Roessner, U., Natera, S. H. A., Hill, C. B., Rupasinghe, T. W. T., & Roessner, U. (2016). Salt-stress induced alterations in the root lipidome of two barley genotypes with contrasting responses to salinity. *Functional Plant Biology*, 43(2), 207–219. <https://doi.org/10.1071/FP15253>
- O'Brien, J., Hayder, H., Zayed, Y., & Peng, C. (2018). Overview of MicroRNA Biogenesis, Mechanisms of Actions, and Circulation. *Frontiers in Endocrinology*, 9(402), 1–12. <https://doi.org/10.3389/fendo.2018.00402>
- Oliveros, J. (2020). Venny. Retrieved May 1, 2020, from <https://bioinfogp.cnb.csic.es/tools/venny/>
- Pertea, G., & Pertea, M. (2020). GFF Utilities: GffRead and GffCompare. *F1000Research*, 9, 304. <https://doi.org/10.12688/f1000research.23297.1>
- Qibin, L. (2020). Mireap [Perl]. Retrieved August 1, 2020, from <https://github.com/liqb/mireap> (Original work published 2014)
- Quillet, A., Saad, C., Ferry, G., Anouar, Y., Vergne, N., Lecroq, T., & Dubessy, C. (2020). Improving Bioinformatics Prediction of microRNA Targets by Ranks Aggregation. *Frontiers in Genetics*, 10(1330), 1–14. <https://doi.org/10.3389/fgene.2019.01330>
- Rao, X., Huang, X., Zhou, Z., & Lin, X. (2013). An improvement of the  $2^{-\Delta\Delta CT}$  method for quantitative real-time polymerase chain reaction data analysis. *Biostatistics, Bioinformatics and Biomathematics*, 3(3), 71–85.
- Redondo-Gómez, S., Mateos-Naranjo, E., Figueroa, M. E., & Davy, A. J. (2010). Salt stimulation of growth and photosynthesis in an extreme halophyte, *Arthrocnemum macrostachyum*. *Plant Biology*, 12(1), 79–87. <https://doi.org/10.1111/j.1438-8677.2009.00207.x>
- Samantary, S. (2002). Biochemical responses of Cr-tolerant and Cr-sensitive mung bean cultivars grown on varying levels of chromium. *Chemosphere*, 47(10), 1065–1072. [https://doi.org/10.1016/S0045-6535\(02\)00091-7](https://doi.org/10.1016/S0045-6535(02)00091-7)

- Sergieiev, I., Alexieiva, V., & Karanov, E. (1997). Effect of spermine, atrazine and combination between them on some endogenous protective systems and stress markers in plants. *Bulgarian Academy of Science*, 53(10), 63–66.
- Shaikh, T. (2017). Taxonomic Study Of The Water Spinach (*Ipomoea Aquatica* Forsk. Convolvulaceae). *NAIRJC*, 3(4), 1–11.
- Shen, C., Huang, Y.-Y., He, C.-T., Zhou, Q., Chen, J.-X., Tan, X., Mubeen, S., Yuan, J.-G., & Yang, Z.-Y. (2017). Comparative analysis of cadmium responsive microRNAs in roots of two *Ipomoea aquatica* Forsk. Cultivars with different cadmium accumulation capacities. *Plant Physiology and Biochemistry: PPB*, 111, 329–339.  
<https://doi.org/10.1016/j.plaphy.2016.12.013>
- Shrivastava, P., & Kumar, R. (2015). Soil salinity: A serious environmental issue and plant growth promoting bacteria as one of the tools for its alleviation. *Saudi Journal of Biological Sciences*, 22(2), 123–131.  
<https://doi.org/10.1016/j.sjbs.2014.12.001>
- Stocks, M. B., Mohorianu, I., Beckers, M., Paicu, C., Moxon, S., Thody, J., Dalmay, T., & Moulton, V. (2018). The UEA sRNA Workbench (version 4.4): A comprehensive suite of tools for analyzing miRNAs and sRNAs. *Bioinformatics (Oxford, England)*, 34(19), 3382–3384.  
<https://doi.org/10.1093/bioinformatics/bty338>
- Tanveer, M., & Ahmed, H. A. I. (2020). ROS Signalling in Modulating Salinity Stress Tolerance in Plants. In M. Hasanuzzaman & M. Tanveer (Eds.), *Salt and Drought Stress Tolerance in Plants: Signaling Networks and Adaptive Mechanisms* (pp. 299–314). Springer International Publishing.  
[https://doi.org/10.1007/978-3-030-40277-8\\_11](https://doi.org/10.1007/978-3-030-40277-8_11)
- Tijssen, P. (1985). Practice and Theory of Enzyme Immunoassays. In *Laboratory Techniques in Biochemistry and Molecular Biology* (1st ed., Vol. 15, p. 548). Elsevier Science.
- Wang, J., Zhu, J., Zhang, Y., Fan, F., Li, W., Wang, F., Zhong, W., Wang, C., & Yang, J. (2018). Comparative transcriptome analysis reveals molecular response to salinity stress of salt-tolerant and sensitive genotypes of indica rice at seedling stage. *Scientific Reports*, 8(1), 1–13.  
<https://doi.org/10.1038/s41598-018-19984-w>
- Xie, F., Stewart, C. N., Taki, F. A., He, Q., Liu, H., & Zhang, B. (2014). High-throughput deep sequencing shows that microRNAs play important roles in switchgrass responses to drought and salinity stress. *Plant Biotechnology Journal*, 12(3), 354–366. <https://doi.org/10.1111/pbi.12142>

- Yang, Z., Li, J.-L., Liu, L.-N., Xie, Q., & Sui, N. (2020). Photosynthetic Regulation Under Salt Stress and Salt-Tolerance Mechanism of Sweet Sorghum. *Frontiers in Plant Science*, *10*(1722), 1–12. <https://doi.org/10.3389/fpls.2019.01722>
- Yu, D., Boughton, B. A., Hill, C. B., Feussner, I., Roessner, U., & Rupasinghe, T. W. T. (2020). Insights Into Oxidized Lipid Modification in Barley Roots as an Adaptation Mechanism to Salinity Stress. *Frontiers in Plant Science*, *11*(1), 1–16. <https://doi.org/10.3389/fpls.2020.00001>

## Appendix

Table 1: Measurements of mineral content in *I. aquatica* (IA) samples and *I. pes-caprae* (IB). Sample labeled C for control, E for Early, and L for Late. Samples were labeled L for leaf and R for Root (IA CL1 is *I. aquatica* control leaf triplicate 1)

Lab Ref	Sample Labels	mg/Kg (ppm)				Percent (%)
		Ca	K	Mg	Na	Chloride
1	IA CL 1	6645.32	20973.1	1852.3	3862.1	1.79
2	IA CL 2	7203.35	16580.2	1817.2	4807.1	1.52
3	IA CL 3	7866.98	16254.5	1946.2	4471.4	1.81
4	IA EL 1	5301.92	22781.0	1979.7	11004.8	2.31
5	IA EL 2	4849.47	21173.3	1986.4	8539.4	2.37
6	IA EL 3	6012.21	21509.6	2088.5	11720.6	2.41
7	IA LL 1	4143.75	19458.8	1663.0	25293.7	6.22
8	IA LL 2	4779.86	19522.7	1470.3	30459.4	7.18
9	IA LL 3	4752.33	25402.3	1761.9	23083.6	4.55
10	IA CR 1	4009.36	12007.4	1125.9	12856.3	1.41
11	IA CR 2	3787.99	10770.9	901.7	13543.6	1.60
12	IA CR 3	3809.08	11771.0	1044.4	12741.6	1.56
13	IA ER 1	2491.95	18270.6	746.6	16774.0	1.94
14	IA ER 2	2360.35	19574.8	747.5	16496.2	2.33
15	IA ER 3	2383.13	19533.1	790.4	16699.3	2.09
16	IA LR 1	3212.66	15940.9	585.6	17568.4	2.87
17	IA LR 2	2609.1	18663.6	629.3	18827.3	2.99
18	IA LR 3	2818.38	16340.0	540.3	15085.8	2.75
19	RL 1 IB	1921.82	24815.5	985.1	25880.0	5.48
20	RL 2 IB	2243.28	24808.3	921.0	24697.4	5.53
21	RL 3 IB	2209.91	23737.3	994.0	24912.6	5.69
22	RC 1 IB	4308.56	26502.8	1103.5	1889.3	0.61
23	RC 2 IB	4644.04	25726.4	1316.9	1962.5	0.82
24	RC 3 IB	4436.22	25581.1	1176.5	1756.3	0.83
25	LL 1 IB	4646.11	16000.7	1029.7	14576.5	4.85

Table 1: Measurements of mineral content in *I. aquatica* (IA) samples and *I. pes-caprae* (IB). Sample labeled C for control, E for Early, and L for Late. Samples were labeled L for leaf and R for Root (IA CL1 is *I. aquatica* control leaf triplicate 1) – (Continued)

Lab Ref	Sample Labels	mg/Kg (ppm)				Percent (%)
		Ca	K	Mg	Na	Chloride
26	LL 2 IB	14112.6	41503.7	3812.5	33324.2	4.64
27	LL 3 IB	4861.89	25128.6	1859.2	20417.0	3.93
28	LC 1 IB	4936.27	22554.2	1571.6	1905.2	0.42
29	LC 2 IB	8299.65	24144.2	2157.1	2950.9	0.56
30	LC 3 IB	8738.31	28206.8	2332.2	3120.2	0.46
31	LE 1 IB	8840.3	25483.6	2017.3	6634.6	1.20
32	LE 2 IB	7827.18	24773.3	2001.5	5054.0	1.38
33	LE 3 IB	6871.63	23767.4	2062.3	3661.7	1.16
34	RE 1 IB	2017.42	28196.9	943.3	17675.6	4.08
35	RE 2 IB	2173.3	28827.1	1092.1	14142.9	3.25
36	RE 3 IB	2309.04	29112.5	1020.1	13491.7	4.24

Table 2: Results of *I. aquatica* bioinformatics analysis representing the percentage of reads remaining after trimming as well as the percentage of reads that were aligned to the Reference genome from each sample. The last column shows the number of reads assembled into non-redundant reads.

	<i>Trimmomatic</i>	<i>HISAT2</i>	<i>StringTie2</i>
<i>Sample</i>	<b>Reads Retained (%)</b>	<b>Reads Aligned (%)</b>	<b>Reads Assembled</b>
<i>Control_Leaf_1</i>	97.06	97.23%	27852
<i>Control_Leaf_2</i>	97.33	96.94%	27852
<i>Control_Leaf_3</i>	96.76	97.04%	27852
<i>Control_Root_1</i>	97.18	89.16%	40410
<i>Control_Root_2</i>	96.90	89.53%	40410
<i>Control_Root_3</i>	97.01	88.43%	40410
<i>Early_Leaf_1</i>	97.12	95.89%	27852
<i>Early_Leaf_2</i>	94.98	95.61%	27852
<i>Early_Leaf_3</i>	97.25	96.06%	27852
<i>Early_Root_1</i>	97.41	88.69%	40410
<i>Early_Root_2</i>	97.48	90.95%	40410
<i>Early_Root_3</i>	97.10	89.79%	40410
<i>Late_Leaf_1</i>	97.32	96.16%	27852
<i>Late_Leaf_2</i>	97.30	95.87%	27852
<i>Late_Leaf_3</i>	96.91	96.83%	27852
<i>Late_Root_1</i>	96.96	87.57%	40410
<i>Late_Root_2</i>	97.70	89.41%	40410
<i>Late_Root_3</i>	97.32	88.28%	40410

Table 3: Results of *I. pes-caprae* bioinformatics analysis representing the percentage of reads remaining after trimming as well as the percentage of reads that were aligned to the Reference genome from each sample. The last column shows the number of reads assembled into non-redundant reads.

	<i>Trimmomatic</i>	<i>HISAT2</i>	<i>StringTie2</i>
<i>Sample</i>	<b>Retained reads (%)</b>	<b>Reads Aligned (%)</b>	<b>Reads Assembled</b>
<i>Control_Leaf_1</i>	98.15	98.35	33119
<i>Control_Leaf_2</i>	98.14	98.38	33119
<i>Control_Leaf_3</i>	98.12	98.36	33119
<i>Control_Root_1</i>	97.46	90.49	45605
<i>Control_Root_2</i>	97.73	89.27	45605
<i>Control_Root_3</i>	97.55	89.18	45605
<i>Early_Leaf_1</i>	97.80	94.65	33119
<i>Early_Leaf_2</i>	95.14	92.70	33119
<i>Early_Leaf_3</i>	97.41	93.87	33119
<i>Early_Root_1</i>	97.58	82.13	45605
<i>Early_Root_2</i>	98.22	88.76	45605
<i>Early_Root_3</i>	97.49	81.9	45605
<i>Late_Leaf_1</i>	97.62	94.68	33119
<i>Late_Leaf_2</i>	98.22	97.93	33119
<i>Late_Leaf_3</i>	98.17	98.16	33119
<i>Late_Root_1</i>	98.20	92.00	45605
<i>Late_Root_2</i>	98.18	86.77	45605
<i>Late_Root_3</i>	98.11	84.74	45605

Table 4: Validation of selected genes using qRT-PCR

	<i>I. aquatica</i> Early		<i>I. aquatica</i> Late		<i>I. pes-caprae</i> Early		<i>I. pes-caprae</i> Late	
	RNA-seq	qPCR	RNA-seq	qPCR	RNA-seq	qPCR	RNA-seq	qPCR
<b>NAC</b>	1.69511602	0.92756494	2.73475868	2.07444127	5.16274998	2.61562169	2.63998625	1.96914594
<b>NAC3-like</b>	1.9	1.27926763	0.9842655	0.88137086	4.26984861	5.58664725	1.84841597	2.07168554
<b>HKT6</b>	0.23863715	-1.2723455	-1.0691276	-2.6830629	3.89355905	14.4987353	0.34399464	5.62489842
<b>HKT-2</b>	0.60322479	-0.9497805	4.21963612	1.60374451	-1.5188326	0.64589123	0.71408732	1.25142173
<b>Osmotin</b>	0.1070466	-0.2128108	3.44088551	2.22739442	6.02758804	7.38484185	6.18228058	5.45065027
<b>Catalase</b>	0.44336878	-0.1423677	2.19361237	0.9762675	0.66359542	2.01668353	2.06475671	3.20536331
<b>AP2/ERF</b>	2.68976998	1.83973853	0.69472769	0.9750843	3.96721652	7.95241976	-1.7975338	1.35847707
<b>CIPK6</b>	-0.2918318	-0.0668186	-0.0456143	0.58152676	2.25552896	3.47852154	0.71883826	1.94122625
<b>SUS3</b>	-0.4476431	1.51454163	1.51544447	0.24311574	2.07586678	2.87647228	1.60309879	1.98267405
<b>KTI2</b>	-0.369762	3.25004832	-1.1114697	2.90570323	5.77987513	10.0456213	2.08842557	4.10232696

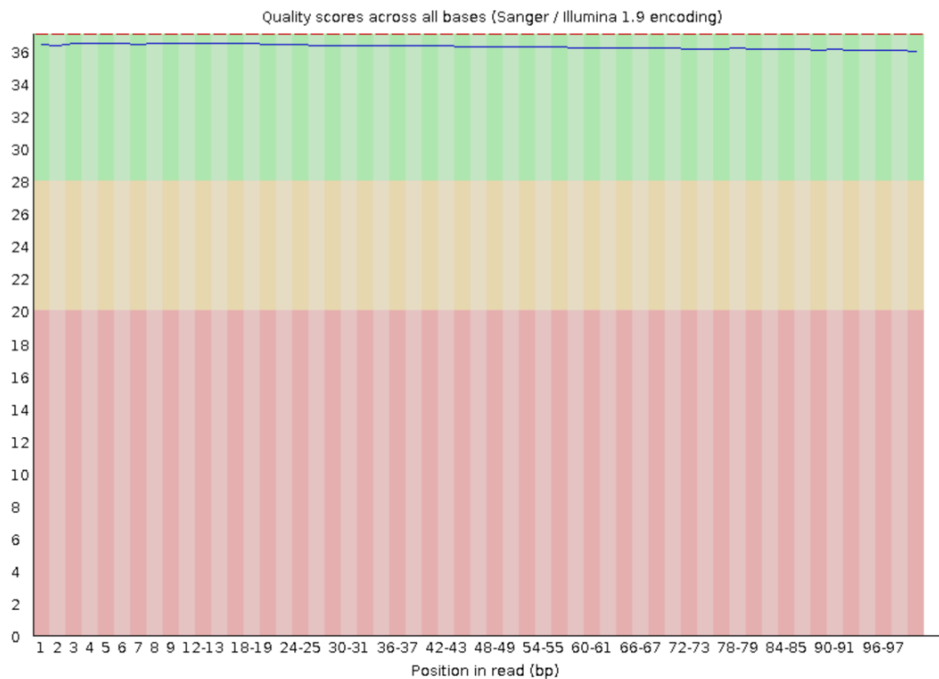


Figure 1: example of FastQC result showing the quality of the sequence along its axis

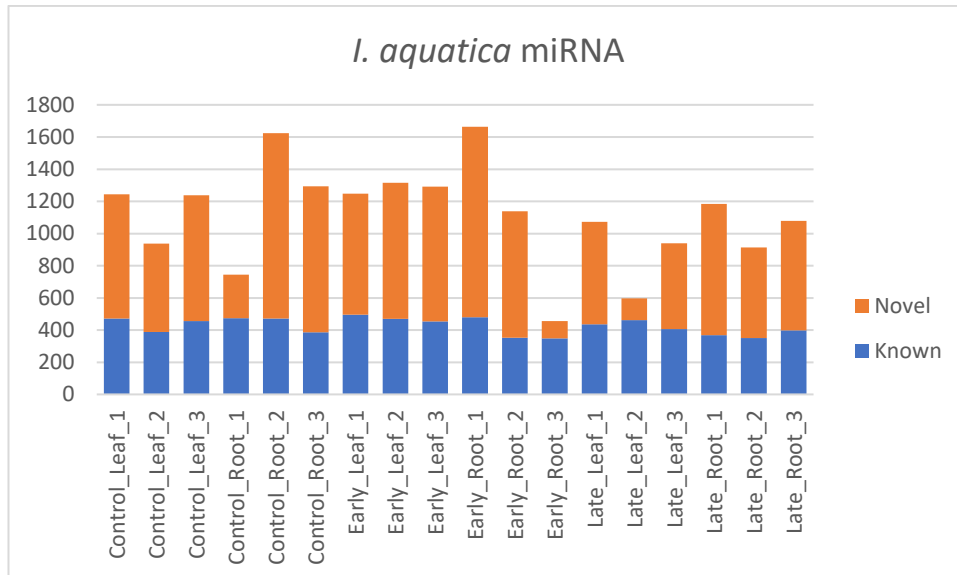


Figure 2: The numbers of known and novel miRNAs identified in *I. aquatica* samples.

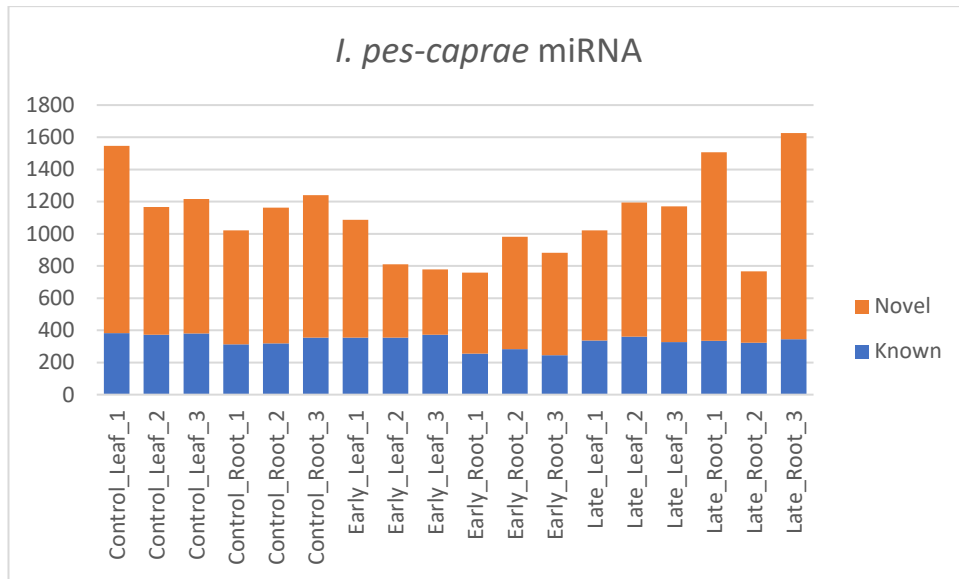


Figure 3: The numbers of known and novel miRNAs identified in *I. pes-caprae* samples.